Korean J. Chem. Eng., 38(2), 386-399 (2021)
DOI: 10.1007/s11814-020-0710-3

pISSN: 0256-1115
eISSN: 1975-7220

Effect of low levels of hydrotropes on micellization of phenothiazine drug

Sulaiman Y. M. Alfaifi*, Dileep Kumar,***,†, Malik Abdul Rub*,****, Farah Khan*****, Naved Azum*,****, Anish Khan*,****, Abdullah M. Asiri*,****, and Hurija Džudžević-Čančar******

*Chemistry Department, Faculty of Science, King Abdulaziz University, Jeddah-21589, Saudi Arabia
**Division of Computational Physics, Institute for Computational Science, Ton Duc Thang University, Ho Chi Minh City, Vietnam
***Faculty of Applied Sciences, Ton Duc Thang University, Ho Chi Minh City, Vietnam
****Center of Excellence for Advanced Materials Research, King Abdulaziz University, Jeddah-21589, Saudi Arabia
*****Department of Chemistry, Aligarh Muslim University, Aligarh-202 002, India
******Department of Natural Science in Pharmacy, Faculty of Pharmacy, University of Sarajevo, Zmaja od Bosne 8, 71 000 Sarajevo, Bosnia and Herzegovina

(*Received 23 June 2020 • Revised 16 October 2020 • Accepted 11 November 2020*)

Abstract−Interactions within mixtures of the phenothiazine drug promethazine hydrochloride (PMH) and cationic hydrotropes *ortho*-toluidine hydrochloride (*o*-TDH) and *para*-toluidine hydrochloride (*p*-TDH) were investigated at different ratios and temperatures via conductometry to understand various physicochemical properties. Critical micelle concentration (*cmc*) was less than values of cmc^{id} (*cmc* in ideal mixed system), indicating significant interaction among the studied constituents in solution mixtures. The *cmc* of pure PMH was also determined by measuring the surface tension for comparison. A variety of micellization thermodynamic parameters (Gibbs free energy [ΔG_m^0], change in standard enthalpy [ΔH_m^0], and change in entropy [ΔS_m^0]) were computed using conductometry. The micellar mole fraction (X_1^{Rb}, X_1^{Rod}, and X_1^{id}) of hydrotropes estimated by various theoretical models (Rubingh, Rodenas, and Motomura) was assessed, and the results showed a greater contribution of hydrotropes in mixed micelles along with their values increasing via an increase in mole fraction (α_1) of hydrotropes (*o*-TDH/*p*-TDH). Negative β values suggest extremely favorable attractive interaction/synergism, as declines occurred in the whole quantity of amphiphile used for the desired purpose, leading to a drop of expenditure along with ecological concern. Obtained activity coefficients (f_1 and f_2) were always beneath unity, meaning nonideality was found between PMH and *o*-TDH/*p*-TDH. Like the conductivity method, the UV-visible and FT-IR techniques also demonstrate the interaction between the PMH and *o*-TDH/*p*-TDH.

Keywords: Promethazine Hydrochloride, Mixed Micelles, Synergism, Conductivity, Thermodynamic Parameters

INTRODUCTION

Surfactants are amphiphiles which include a polar hydrophilic group and nonpolar hydrophobic group in a single molecule and are capable of a variety of chemical interactions [1]. Understanding self-association characteristics of amphiphiles such as surfactants is of immense significance because of their utilization in a broad range of both research and industrial applications [2]. Nearly all types of surfactants self-assemble in aqueous and other solutions at or above specific concentrations into micelles, and the concentration at which micelle formation initiates is called the critical micelle concentration (*cmc*) [3-7]. Surfactant micelles are vital in pharmaceuticals as their palisade layers can solubilize and transport hydrophobic drugs [8].

There has been recent great research interest in exploring the self-association potential of amphiphilic drugs, which show surface activity akin to typical surfactants [9-11]. The study of amphiphile-additive mixed systems has been especially significant as they are capable of forming mixed aggregates efficiently, at low cost, and with high mixed micelle surface activity. A mixed system can better demonstrate interfaces and show colloidal assets different from those of either single constituent. As a result, in pharmaceutical sciences, mixed micelle systems are employed to enhance the absorption of a variety of drugs in humans [12,13].

Most natural surfactants are water-soluble and used for the solubilization of hydrophobic compounds [2]. Akin to surfactants, hydrotropic agents called hydrotropes are freely soluble in the aqueous and nonaqueous solvent and, at a sufficiently higher concentration than usual surfactants, start to form a stack-type association at a minimum hydrotropic concentration (*mhc*) analogous to micelle formation of surfactant at the *cmc* [14,15]. Hydrotropes significantly increase the solubility of organic constituents such as hydrophobic drugs in aqueous and nonaqueous systems under virtually normal states [14,15]. The structure of hydrotropic agents is like surfactants since a hydrophobic and a hydrophilic exist within a monomer of a hydrotrope; however, the hydrotrope hydrophobicity is usually found to be much below as compared with usual surfactant. Regardless of the likeness of hydrotrope and surfactant nature in decreasing the surface tension, micropolarity, conductivity, and so on [2], there are several variances amid surfactant and

†To whom correspondence should be addressed.
E-mail: dileepkumar@tdtu.edu.vn

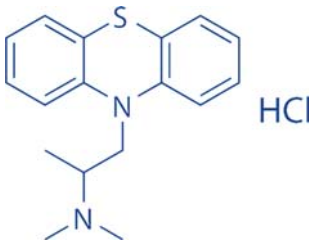

Scheme 1. Structure of promethazine hydrochloride (PMH).

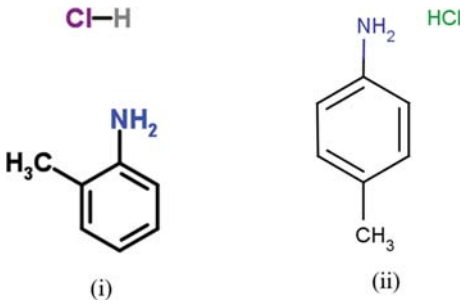

Scheme 2. Structure of cationic hydrotropes (i) *ortho*-toluidine hydrochloride (*o*-TDH) (ii) *para*-toluidine hydrochloride (*p*-TDH).

hydrotrope, i.e., *mhc* value is achieved much higher as compared with the *cmc* value. As a result of the small hydrophobic parts as well as the high concentration required for solubilization, some have well-thought-out them to be distinct from usual surfactants but both types of aggregates (*cmc* and *mhc*) can dissolve insoluble hydrophobic molecules [16]. Some hydrotropes have also been reported to improve the solubility of some aromatic molecules by nearly 1,000-fold [17], which can be effectively exploited in separations as well as distillations of nearby boiling materials.

As a result of the technological and biological advantages demonstrated by mixed micelles in research, industrial, and pharmaceutical applications, new amphiphile and additive mixtures, rather than single amphiphile systems, can be created for drug delivery [18]. In this study, we analyzed the amphiphilic drug promethazine hydrochloride (PMH) (Scheme 1) found in certain phenothiazine drugs. It is employed to cure allergy symptoms, provide sleep support, and treat drug allergic reactions. This class of drugs causes some unwanted effects and therefore, for safe delivery, requires a carrier such as a cationic hydrotrope. Along with, it is well known that cationic amphiphiles are relatively toxic; however, they are sometimes used in pharmaceutics as their effects outweigh their toxicity effects [2].

The structure of PMH is comprised of a rigid, planar, tricyclic ring system and a short hydrocarbon chain with a terminal N molecule attached; the molecules usually associate in smaller assemblies up to 15 monomers [19]. At lower pH, the tertiary nitrogen atom is protonated and attains a positive charge, and at higher pH it becomes deprotonated or neutral.

The aggregation of amphiphilic materials consistently demonstrates a variety of physicochemical characteristics. The head group region of micelles offers a highly polar atmosphere, whereas the central portion exhibits low polarity. Therefore, the micelles are proficient in capturing hydrophobic drugs in their interior and thereby increase bioavailability and the solubility of the drug in water [20,21].

In this study, the mixed micellization behavior and composition of the cationic drug PMH combined with two different cationic hydrotropes, *o*-TDH and *p*-TDH (Scheme 2), were studied at various temperatures by the conductometric method. Irrespective of conductivity measurement, UV-visible and FTIR investigation was also conducted to further confirm PMH and *o*-TDH/*p*-TDH interaction. Determining electrical conductivity is a unique and straightforward method to determine the association behavior of singular amphiphiles as well as mixtures of amphiphiles in the presence of different additives. This approach is well-suited to measuring ion-ion as well as ion-solvent interactions in mixed solution systems. Significant PMH thermodynamic properties, the result of the solution composition and temperature, require consideration of the effect of hydrotropes on PMH association phenomena. Prepared stock solutions of PMH were added to different concentrations of cationic *o*-TDH and *p*-TDH well below their *cmc* values at different temperatures. By determining the *cmc* via the conductometric method, we can assess various physicochemical parameters that account for the micellization of PMH and selected cations.

EXPERIMENTAL METHODS

1. Chemicals

Separate stock solutions of PMH (98%; Sigma, USA) and hydrotropes *o*-TDH and *p*-TDH (99%; Fluka, Switzerland), as well as their mixtures, were prepared in double-distilled and deionized water with specific conductivity of 1-6 μS cm^{-1}.

2. Conductometric Technique

The conductivity value of experimental solutions was measured by a digital conductivity meter (Jenway 4510, UK) with a dip cell constant of 1.0 cm^{-1} and a precision of approximately ±0.5%. To maintain the desired system temperature, a circulating-thermostat water bath was used (error of ±0.2 K). The current conductivity experiment was performed at five different temperatures: 293.15, 298.15, 303.15, 308.15, and 313.15 K. For PMH-hydrotrope mixtures, specific concentrations of the hydrotrope solutions were employed as a solvent in place of deionized H_2O. After the completion of the experiment, graphs were plotted of specific conductance (κ) vs. [PMH] in the absence as well as attendance of hydrotropes. The *cmc* of the studied system was identified as the concentration of PMH where the plot changed slope.

3. Surface Tension Measurement

Surface tension (γ) measurements of pure PMH solutions were performed using a 701 Attension tensiometer (Sigma, Germany) by the detached ring method. Detailed methods of measuring surface tension are provided in [13]. The γ were evaluated by adding prepared PMH stock solution to water at 293.15 K. Analysis was repeated until γ of PMH solutions were constant. The *cmc* value of pure PMH was obtained from the cut-off spot in a plot of the γ vs. logarithm concentration (log[PMH]). Temperature error was ±0.2 K, and the relative uncertainty in PMH *cmc* values was approximately ±3%.

4. UV-visible Absorption Measurements

UV-visible spectroscopic studies were accomplished to figure out the PMH–*o*-TDH/*p*-TDH hydrotrope interactions in an aqueous system. The absorbance spectra were noted on a Thermo Scientific, Evolution 300 UV-visible spectrometer having a 1 cm path length quartz cuvette. Herein, the effect of increasing concentration *o*-TDH/*p*-TDH hydrotrope was seen on the absorption spectra of the fixed concentration of PMH drug (0.25 mmol·kg^{-1}). The stock solutions of *o*-TDH/*p*-TDH hydrotrope were prepared in the presence of a 0.25 mmol·kg^{-1} PMH to avoid the dilution effects during titrations.

5. FT-IR Spectroscopy

A Thermo Scientific NICOLET iS50 FT-IR spectrometer (Madison, USA) was employed to record the FT-IR spectra of pure PMH and *o*-TDH/*p*-TDH and their mixture in equally ratio in an aqueous system in the wavelength range of 4,000 to 400 cm^{-1}. However, for clarity of the graph only a certain range of the wavelength is shown in the graph. The spectrum of water was subtracted from wholly achieved spectra of the employed system.

RESULTS AND DISCUSSION

1. Effect of Hydrotrope (*o*-TDH/*p*-TDH) on the *cmc* of PMH Drug

Conductometry has long been used as a unique tool to evaluate significant physical parameters in the determination of *cmc* values of surface-active amphiphiles. The conductivity technique is a simple, reliable, and most useful technique for studying aggregation phenomena of ionic amphiphiles. The conductivity of surface-active amphiphile solutions in water increased linearly as the concentration of amphiphiles increased. However, above a specific amphiphile concentration, conductivity values decreased, as observed by a change in plot slope of conductance vs. amphiphile concentration. This indicates that the added amphiphiles have started to form associate structures called micelles [2]. The actual *cmc* is obtained from the cut-off point in the specific conductance (κ) against [amphiphiles] profile. Fig. 1 shows the plots of specific conductance (κ) vs. the [PMH] across a range of mole fractions (α_1) of *o*-TDH at 293.15 K.

The pKa value of pure PMH was 9.1, and in the aqueous system used, this drug becomes positively charged [22]. The *cmc* values of entire systems (PMH alone and its mixtures with hydrotropes) and *mhc* values of hydrotropes at numerous temperatures are in Fig. 2 and Tables S1 and S2 (Supplementary Material). The specific conductivity (κ) data of PMH, *o*-TDH/*p*-TDH as well as PMH–*o*-TDH/*p*-TDH mixtures of different mole fraction (α_1) of *o*-TDH/*p*-TDH at different studied temperatures are shown in Tables S3 and S15 (Supplementary Material). The *cmc* and *mhc* values of singular PMH and hydrotropes (*o*-TDH/*p*-TDH), respectively, agree with values obtained previously [8,19,23-26]. The *mhc* values of singular hydrotropes (*o*-TDH/*p*-TDH) were found to be less than half of the PMH *cmc* value, likely because the presence of the tricyclic ring in PMH makes them difficult to incorporate into micellar shape (somewhat spherical) than the hydrotropes [10,23]. Therefore, both employed hydrotropes start the self-association at lower concentration than PMH. The *cmc* value of PMH alone was also evaluated by the tensiometric method at 293.15 K for comparison with conductometry results. The evaluated *cmc* value of PMH through surface measurement is shown in Fig. 3. The *cmc* value of PMH was very similar in both techniques (36.51 mmol·

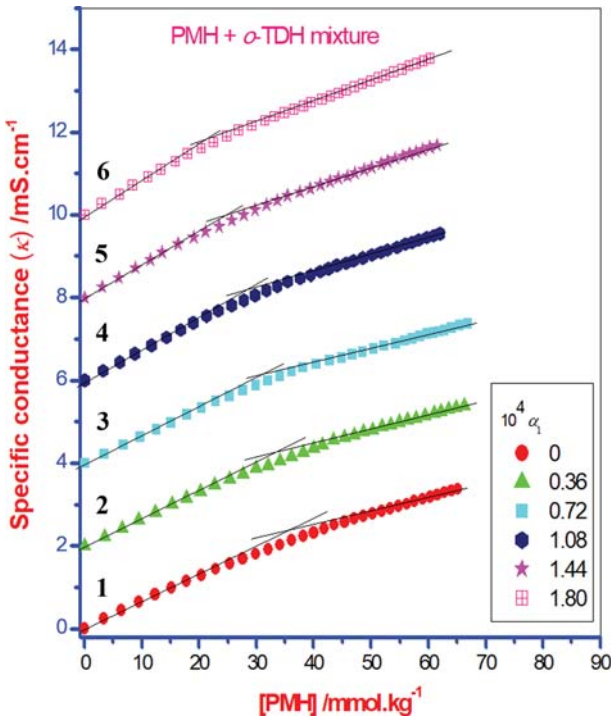

Fig. 1. The plots of specific conductance (κ) versus [PMH] in a range of mole fractions (α_1) of *o*-TDH at 293.15 K. Plots 2, 3, 4, 5, and 6 are shifted successively by 2 scale units (mS cm^{-1}).

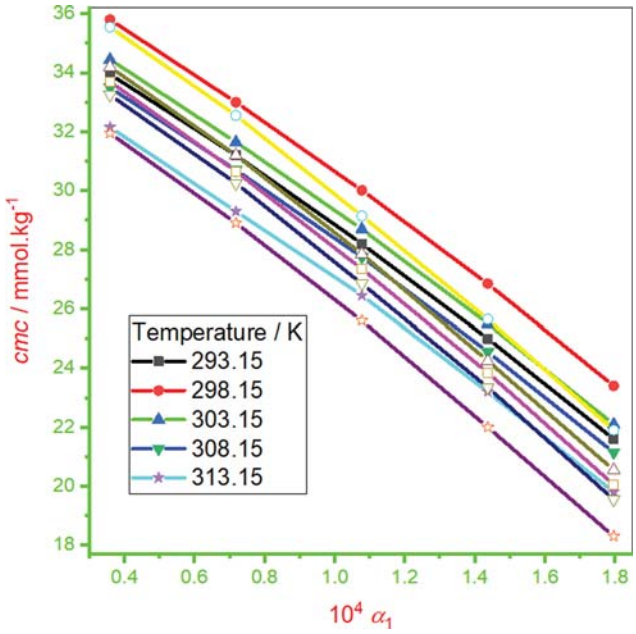

Fig. 2. Variation of *cmc* of PMH-hydrotrope (*o*-TDH/*p*-TDH) mixture versus mole fraction (α_1) of hydrotrope (filled symbols and open symbols represent the PMH–*o*-TDH and PMH–*p*-TDH mixtures, respectively).

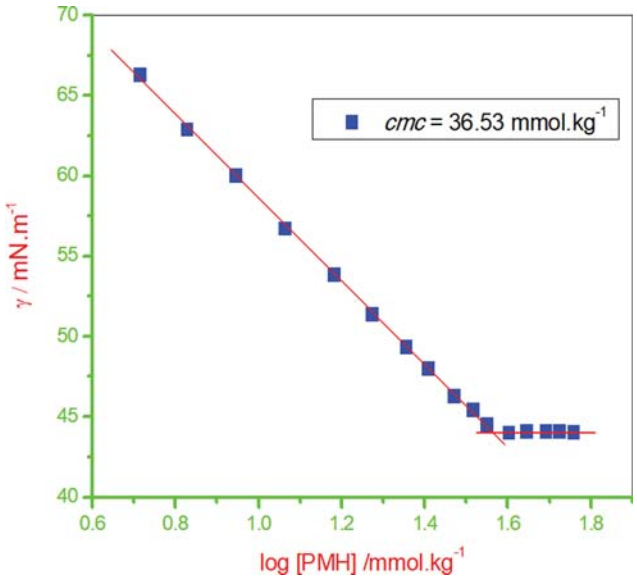

Fig. 3. Surface tension (γ) versus concentration of pure PMH in aqueous solution at 293.15 K.

kg^{-1} was obtained via the conductometric method and 36.53 mmol·kg^{-1} was found by surface tension method). By the fluorescence method, *cmc* value of PMH was earlier obtained to be 39.265 mmol·kg^{-1} by Mahajan et al. [23], which was also in good conformity with our obtained *cmc* value of PMH (38.31 mmol·kg^{-1} at 298.15 K) via the conductivity method.

Fig. 2 and Tables S1 and S2 (Supplementary Material) show the impact of different mole fractions (α_1) of hydrotropes as well as temperature on the PMH *cmc* value. Here, different ratios signify the different mole fractions of hydrotropes (α_1) in the mixed system of PMH and *o*-TDH/*p*-TDH solutions. Herein, α_1=mole fraction of *o*-TDH/*p*-TDH (first constituent) and α_2=mole fraction of PMH (here considered the second constituent) and sum of α_1 and α_2 is equal to 1. The employed concentrations of *o*-TDH/*p*-TDH were much less than their *mhc* values; therefore, it is concluded that a part of added *o*-TDH/*p*-TDH monomers only formed the mixed micelles with the PMH monomers and the remainder of hydrotrope monomers exist as free monomers in the solvent. The *cmc* value of PMH decreased in the presence of *o*-TDH/*p*-TDH at all temperatures. In addition, the *cmc* value of PMH further decreased as the α_1 value of *o*-TDH/*p*-TDH increased, showing that mixed micellization in solution mixtures occurred because the *cmc* of PMH decreased.

The obtained *cmc* values of mixed systems were close to the value of *cmc* of both single components. The decrease in PMH *cmc* values was due to the presence of *o*-TDH/*p*-TDH, understanding that the process of mixed micellization occurs because of attractive interactions between involved molecules. Added hydrotropes attached directly through the (hydrophilic) head group of cationic PMH; hence, repulsions among the PMH monomers head group decreased. Accordingly, the initiation of associations in drug/hydrotrope mixtures occurred at a lower concentration [2]. The additives which more efficiently reduce the *cmc* value of amphiphiles were generally solubilized on the micellar core exterior. Herein, the extent of *cmc* decrease of PMH can be represented as *p*-TDH>*o*-TDH; however, the employed mole fraction of both types of hydrotropes was the same, and both hydrotropes are equally hydrophobic. The occurrence of the ortho (besides the head) -CH_3 group in *o*-TDH likely caused steric hindrance; consequently, its effect on reducing PMH *cmc* was slightly less than that of *p*-TDH. Landázuri et al. [27] also reported the similar behavior of effect ortho and para derivate of fluorobenzoic on association and adsorption phenomena of hexadecyltrimethylammonium surfactant.

The level of interaction among the studied constituents can be judged by the deviation of experimentally determined *cmc* values through their corresponding cmc^{id} (ideal *cmc*) values, determined theoretically. The cmc^{id} values of the PMH-hydrotrope mixed system of all studied mole fractions of *p*-TDH and *o*-TDH were assessed using Clint's equation [28]:

$$\frac{1}{cmc^{id}} = \frac{\alpha_1}{cmc_1} + \frac{\alpha_2}{cmc_2} \quad (1)$$

Here, cmc_1=*mhc* of the *o*-TDH/*p*-TDH and α_1 is their mole fraction, cmc_2=*cmc* of singular PMH, and α_2 is their mole fraction. This equation shows that under ideal behavior, the interactions among the studied ingredients are zero or null. Applying Clint's theory [28], after comparing experimental *cmc* values and cmc^{id}, it is concluded that systems (solution mixtures) either behave like an ideal or non-ideal system. In our case, experimental *cmc* values were always lower than the cmc^{id}, implying that the systems showed non-ideal behavior along with attractive interaction amid the constituents.

In any case, for the study of interactions between constituents, if $cmc>cmc^{id}$, the system shows antagonistic behavior while $cmc<cmc^{id}$ means the system shows synergistic behavior or attractive interaction. As our results show $cmc^{id}>cmc$ (Fig. 2 and Tables S1 and S2 (Supplementary Material)), synergistic or attractive interactions occurred between the constituents. By mixing hydrotrope into the PMH solution, the intercalation of the *o*-TDH/*p*-TDH monomers takes place among drug micelles. This decreases the repulsive interactions among the PMH head groups, causing an increase in hydrophobicity in a mixed system [29]. The mixed micelles formed by PMH and *p*-TDH showed greater hydrophobicity than PMH and *o*-TDH mixtures, meaning the PMH and *p*-TDH system demonstrated higher non-ideal behavior (as obtained experiment *cmc* values of PMH−*p*-TDH mixtures deviated more from ideal *cmc* values as compared with PMH−*o*-TDH mixtures) as well as more interactions with each other [32]. The employed PMH drug is openly soluble in aqueous and non-aqueous system and forms micelles. But, as is shown from its value of *cmc* (38.31 mmol·kg^{-1}), it is not hydrophobic enough to act as its own carrier. It is well known that most of the drugs have some unwanted effects, and the use of high doge (concentration) in practical applications may lead to adverse side effects and high toxicity. The use of a higher concentration of drug means more unwanted effects. Therefore, here hydrotropes are used as a carrier for such drugs and their mixed micelles with the drug would increase drug bioavailability and, as a result, a low concentration of drug would be required for effective treatment because *cmc* of mixtures are decreased.

2. Effect of Temperature

By simply increasing the temperature, two opposing effects simultaneously affected the micellization behavior of any amphiphile: (a) hydration of the hydrophilic portion (head groups) of molecules was reduced with an increase in temperature, which eased the association accordingly and decreased *cmc*, and (b) the thermal motion of the amphiphile monomers increased through an increase in temperature; therefore, the start of micellization was delayed to some extent, resulting in higher *cmc*. The magnitude of these two opposing conditions determines the variance of *cmc* with temperature [30]. A continuous decrease in *cmc* values with increasing temperature has been reported in nonionic compounds because of an increase in hydrophobicity, and *cmc* reduction with increases in temperature followed by an increase in *cmc* after a certain temperature means showed minima has been reported for ionic compounds. In contrast, a continuous rise in *cmc* with temperature has also been reported in ionic amphiphiles [2].

The variation of *cmc* (*mhc* in case of pure hydrotrope) with temperature change in the case of individual constituents (PMH and *o*-TDH/*p*-TDH) and their mixed systems in different mole fractions are in Fig. 2 and Tables S1 and S2 (Supplementary Material). For individual hydrotropes (*o*-TDH/*p*-TDH), *mhc* increased reliably with increasing temperature. The increase in *mhc* with temperature shows the superiority of hydrophilic hydration, because the thermal motion of the water, as well as hydrotrope molecules, increased, which disorders the H_2O assembly near the hydrophobic part of the monomers. In PMH alone and PMH+*o*-TDH/*p*-TDH mixtures, the *cmc* showed peak behavior with temperature, i.e., reached maxima at 298.15 K. The *cmc* versus temperature plot for PMH+*o*-TDH/*p*-TDH mixtures show similar behavior to that of pure PMH, since very low mole fractions of *o*-TDH/*p*-TDH were added to the solution. The *cmc* value of PMH and PMH+*o*-TDH/*p*-TDH mixtures at all mole fractions increased as temperature rose from 293.15 K to 298.15 K, due to the reduction in dehydration of the hydrophilic (head groups) portion. Nevertheless, as temperature increased from 298.15 to 303.15 K, the *cmc* of systems decreased, and at 308.15 K, their value further reduced. This indicates that at higher temperatures, there was a significant reduction in hydrophilic hydration, signifying that water allied through the tricyclic ring portion of PMH was released. This would increase the hydrophobicity of PMH molecules, a critical feature in micelle formation. Similar *cmc*-temperature curves have been obtained in drug-additive systems [31,32].

In the present study, our purpose was to examine the association behavior of PMH through variation of temperature. The variation of temperature 20 K with a regular interval of 5 K aided our goal as obtained *cmc* value displayed peaked behavior via variation of temperature having the peak at 298.15 K, and this temperature is found to be beneath the human body temperature. Overall, it is concluded that the *cmc* of PMH-hydrotrope mixture (as mixtures *cmc* values were obtained less than individual PMH *cmc* value) would not be above the *cmc* value of individual PMH when introduced in the body means their value should be lower than that acquired at 298.15 K as is obvious from the pattern appeared in *cmc*-temperature plot.

As specified in the introduction section this class of the drug shows some side effects and hence is employed with carriers to minimize their side effects. Even though, PMH drug is freely soluble in both aqueous/non-aqueous solutions, which indorses association. As clear from PMH *cmc* value (38.31 $mmol \cdot kg^{-1}$ at 298.15 K) that PMH was not hydrophobic enough to act as their carrier. Here, in the current study, we aimed to adjust the concentrations of both the drug and carrier in a manner that the prepared mixed system of drug and carrier shows acceptable results with minimum side effects. From obtained results, it is obvious that even extremely small quantities of hydrotrope (*o*-TDH/*p*-TDH) cause mixed micelle formation in the solution mixtures of PMH-hydrotrope, decreasing the *cmc* value of PMH more than 25%. The use of higher hydrotrope (*o*-TDH/*p*-TDH) concentrations altogether means a different situation where hydrotrope micelles work as drug carriers but here only hydrotrope in monomeric form is used as a drug carrier.

3. Degree of Micelle Ionization (g)

The overall obtained results have relevance in model drug delivery, but from this study we cannot conclude any direct evidence for drug delivery. This study is based on the physicochemical interaction of drugs and their possible carrier using various theoretical models and is important from the viewpoint that hydrotrope is also used as drug carriers. Initially, specific conductivity (κ) values for ionic amphiphiles increased as their concentration increased because the mobility of liberated ions rises as solute increases. However, after a particular concentration of solute was added, the specific conductivity (κ) started decreasing. Therefore, in the plot of κ versus [amphiphile concentration], a cut-off point, the *cmc*, was obtained. The slope before *cmc* was higher than the slope after, as the mobility of monomeric amphiphiles was greater than formed micelles after *cmc* was reached [2]. Through the growth of the formed micelles, the number of counter ions binding with the stern layer declined, indicating micelle ionization was occurring.

The degree of micelle ionization (g) was evaluated via the ratio of the slope after the start of micellization (S_2) and before the start of micellization (S_1) using: $g=S_2/S_1$ [33,34]. This is a common way to evaluate the degree of micelle ionization (g) because of simplicity and good valuation potential. The ions attached to micelles become incapable of being charge carriers. The loss of counterion ionization is equal to the number of ions attached to the micelles. The value of g declined through a rise in salt concentration as well as through micellar growth, and when temperature increased, the *cmc* values rose and micellar growth decreased [35,36]. Consequently, through the rise in temperature, a rise in g values is predictable, a phenomenon also detected in ionic amphiphiles [37]. The accuracy of the valuation of g value via conductivity way was further approved by g value evaluated with the ion-selective electrode technique by other researchers [38,39]. The extent of the g value is important to differentiate the micellar performance of the amphiphiles. The micelle's stability, as well as their shape change from sphere-shaped to rod-like assembly, mainly depends on the viscoelastic behavior of the amphiphile and it is directly related to the g value [39]. Additionally, in genuine use where the micellar surface charge plays a crucial job such as DNA transportation; therefore, the g value valuation is significant [40]. The reaction rate of natural organic substrates with hydrophilic molecules holding the bind-

ing capacity to the micelle is fundamentally reliant on the g value [39].

The values of g obtained in this study (singular and mixed amphiphile systems) are in Tables S1 and S2 (Supplementary Material), which also show that for a mixed system of PMH and *o*-TDH/*p*-TDH, the g value declined consistently as α_1 of the *o*-TDH/*p*-TDH increased in the systems. This suggests a counter ion ionization took place, meaning an increase of counter ion binding occurred through the micelle stern layer. The decrease in g values with increasing α_1 of the *o*-TDH/*p*-TDH shows strong binding of the *o*-TDH/*p*-TDH molecules with the PMH drug micellar surface. This resulted in a decrease of the electrostatic repulsions which continued to increase with increasing mole fraction. In mixtures of constituents (PMH+*o*-TDH/*p*-TDH), the values of g were close to singular PMH g values, because the drug is the principal constituent of the mixture. The value of g was lower for PMH+*p*-TDH mixtures than PMH+*o*-TDH mixtures (Tables S1 and S2 (Supplementary Material)).

The obtained value of g of mixed systems was found lower as compared with g value of pure PMH drug showing the interaction between PMH and *o*-TDH/*p*-TDH. It is reported that the higher the g value, the higher will be the *cmc* value [2]. Therefore, it is concluded that *cmc* is directly proportional to the g, which means lower *cmc* corresponds to lower g or vice versa. As *cmc* value of mixed systems decreased with an increase of α_1 of *o*-TDH/*p*-TDH, the g value also decreased with an increase of α_1 (i.e., the interaction between PMH and *o*-TDH/*p*-TDH enhanced with α_1 of *o*-TDH/*p*-TDH). Lower *cmc* of the mixed system means a lesser quantity of drug-hydrotrope mixtures is needed for a particular purpose, as compared to the quantity of the pure drug. In quantity, less use of the drug for any application carries less risk of side effects and decreased toxicity. As shown in our case, as *cmc* value of the mixed system decreases, in that case the g value also decreases; therefore, the obtained lesser g value, also confirming the start of micellization at a lower concentration.

4. Thermodynamics of Micellization

Amphiphilic solution systems may be composed of two different phases: (i) ordered phase, i.e., micellar phase, and (ii) disordered phase, i.e., free amphiphile monomers. The polar head groups of molecules tend to repel one another as they maintain similar charges as well as dipole moments. However, nearby monomers must persist enough collectively to prevent water from gaining entrance to the hydrophobic micellar core. Using Eqs. (2)-(4), Gibbs free energy (ΔG_m^0), enthalpy (ΔH_m^0), and entropy (ΔS_m^0), respectively, of currently studied systems, were determined, as in [41,42].

$$\Delta G_m^0 = (2-g)RT\ln X_{cmc} \tag{2}$$

$$\Delta H_m^0 = -(2-g)RT^2\left[\frac{\partial \ln X_{cmc}}{\partial T}\right] \tag{3}$$

$$\Delta S_m^0 = \frac{\Delta H_m^0 - \Delta G_m^0}{T} \tag{4}$$

Here, X_{cmc}=*cmc* value in mole fraction and R=gas constant. As stated earlier, in place of *cmc*, *mhc* is used in the case of singular hydrotropes. The obtained value of all thermodynamic parameters is presented in Figs. 4 and 5 and Tables S1 and S2 (Supplementary Material).

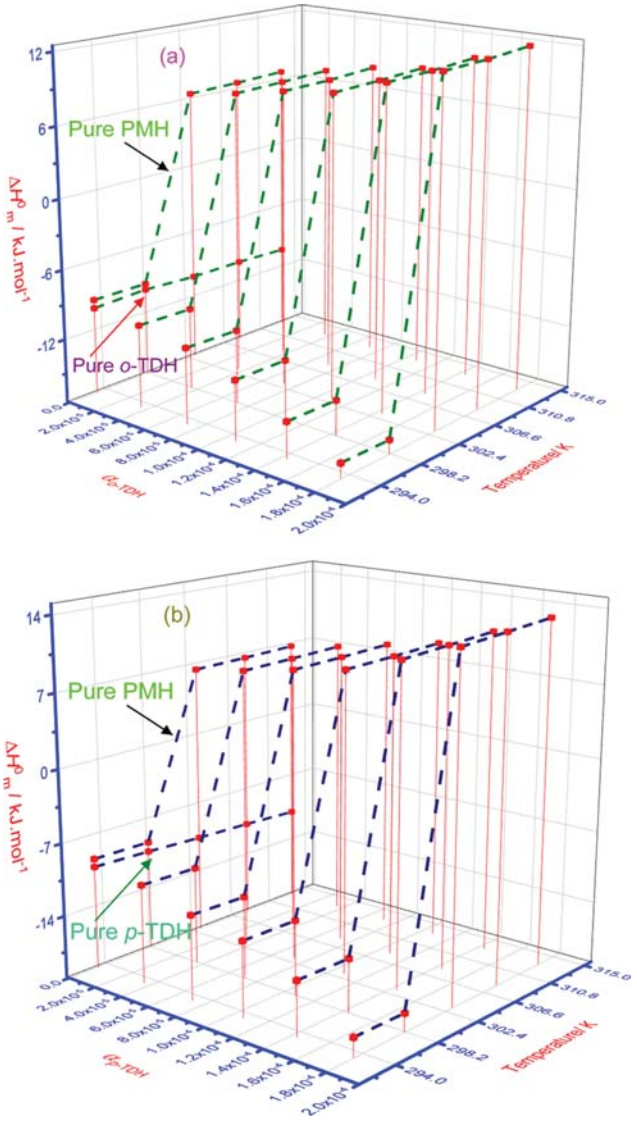

Fig. 4. Effect of mole fraction (α_1) and temperature on ΔH_m^0 of (a) PMH−*o*-TDH, and (b) PMH−*p*-TDH mixtures.

The values of ΔG_m^0 for all systems were negative, showing reaction spontaneity. In addition, their values varied only slightly through temperature changes (Tables S1 and S2 (Supplementary Material)). For pure PMH [24,43] and pure hydrotropes [25,44] the ΔG_m^0 values were in agreement with earlier reported values. A greater negative ΔG_m^0 was found for pure *o*-TDH/*p*-TDH than for pure PMH, indicating that the micellization phenomena in hydrotropes was more spontaneous. This could be because the rigid, hydrophobic structure of PMH makes association initiation difficult. Furthermore, the ΔG_m^0 of the pure drug PMH was less negative than that for all mixed systems, but their value for mixed systems was found to be close of the drug ΔG_m^0 value because a small quantity (mole fraction) of hydrotrope was employed in the system, indicating that mixed systems micellization is more spontaneous than singular PMH micellization. Accordingly, we conclude that *o*-TDH/*p*-TDH has exceptional drug binding aptitude and can be a source of

an improved drug delivery vehicle.

It was also found that with an increase in α_1 of the hydrotropes in the system, the negative value of ΔG_m^0 also increased, reaching its maximum at maximum α_1 (Tables S1 and S2 (Supplementary Material)). The highest negative ΔG_m^0 value and the highest negative value of β (interaction parameter, discussed in a later section) were obtained at the highest mole fraction of *o*-TDH/*p*-TDH, demonstrating that the aggregation takes place more favorably at highest α_1, via increasing interaction between the studied constituents after mixing. Apart from this, the ΔG_m^0 values for PMH–*p*-TDH mixtures were higher at all studied α_1 than for PMH–*o*-TDH mixtures, indicating that micellization phenomena in PMH–*p*-TDH mixed systems were more spontaneous than in the PMH–*o*-TDH mixed system (Tables S1 and S2 (Supplementary Material)).

Enthalpy change of micellization (ΔH_m^0) was evaluated via Eq. (3) and values of all studied systems are listed in Fig. 4. For the pure hydrotrope, the ΔH_m^0 values were negative throughout the entire studied range of temperatures, indicating that the micellization phenomenon in pure hydrotropes is exothermic [45]. Negative ΔH_m^0 values signify that the London-dispersion interactions are a primary force, while positive values of ΔH_m^0 indicate the hydrophobic interactions are the main force during micellization [46]. The negative ΔH_m^0 values attained for the hydrotrope were possibly the result of decreased H-bonds among the water particles, consequently requiring less energy to disintegrate the H_2O clusters near the hydrocarbon chain in the systems. The negative value of ΔH_m^0 in hydrotropes did not change significantly with temperature, and only somewhat increased, signifying little variation in the hydrocarbon portion of the surrounding *o*-TDH/*p*-TDH molecules through the temperature change [44].

For pure PMH and PMH+*o*-TDH/*p*-TDH mixtures in all ratios at lower temperatures (293.15 as well as 298.15 K), the ΔH_m^0 values were negative; however, at higher temperature (303.15, 308.15, and 313.15 K), their values were positive. This indicates that for individual PMH and PMH+*o*-TDH/*p*-TDH mixtures at lower temperature, the micellization process was exothermic, and at higher temperature systems become endothermic [47]. In this case, the obtained negative ΔH_m^0 values are due to the destruction of H-bonds in H_2O molecules near the hydrophobic structure of the studied component. In contrast, at elevated temperature, the unusual positive ΔH_m^0 values were possibly due to dehydration near the hydrophobic structure of monomers, signifying that the hydrophobic interactions were a primary force during the association. The endothermic reaction (positive value of ΔH_m^0) at higher temperature in pure PMH and the PMH+*o*-TDH/*p*-TDH mixed systems was probably due to dehydration from the tricyclic portion of PMH. This shows that the expulsion of H_2O molecules from the hydrophobic PMH structure decreased the *cmc* [48].

The entropy changes of micellization (ΔS_m^0) were calculated using Eq. (4) and are shown in Fig. 5. For singular hydrotrope, the ΔS_m^0 values were positive at every employed temperature; however, their values decreased as temperature increased. This shows that self-aggregation was poorer at increased temperature as molecular motion increased, indicating dehydration of the hydrotrope hydrophobic portion decreased, barring micelle formation to some extent

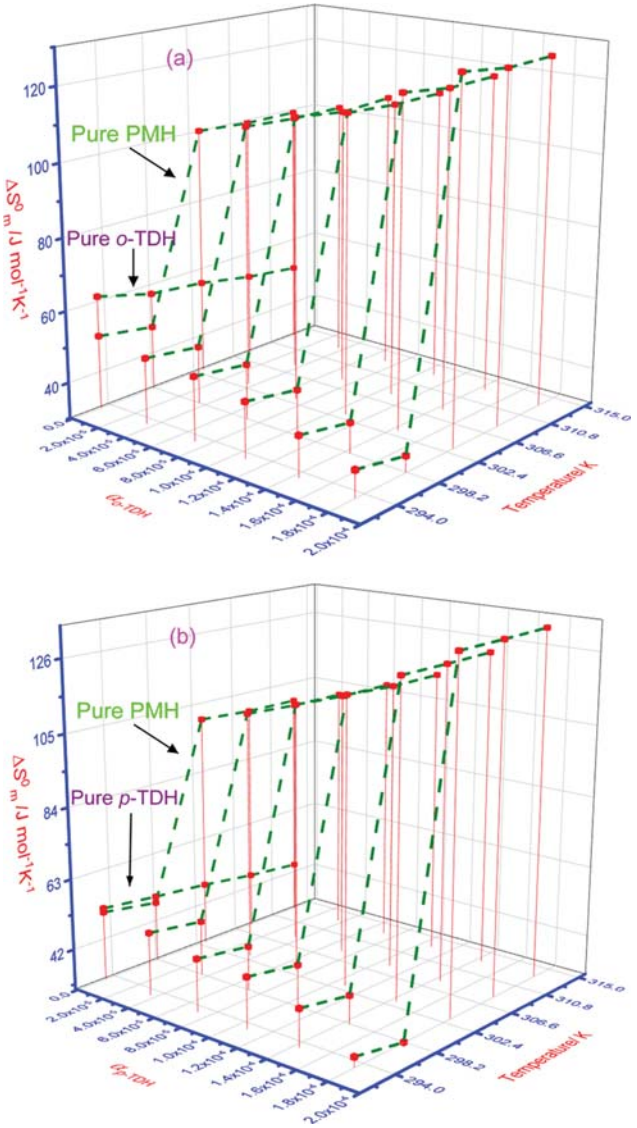

Fig. 5. Effect of mole fraction (α_1) and temperature on ΔS_m^0 of (a) PMH–*o*-TDH, and (b) PMH–*p*-TDH mixtures.

[49]. Consequently, the *cmc* values of singular *o*-TDH/*p*-TDH increased with temperature increase.

However, for PMH and PMH+*o*-TDH/*p*-TDH mixtures, the values of ΔS_m^0 were positive at all temperatures but show dissimilar behavior from the traditional amphiphiles. At lower temperature (293.15 and 298.15 K), the values of ΔS_m^0 were lower but as the temperature rose to 303.15 K and above (308.15 and 313.15 K), the positive values increased dramatically (Fig. 5). At lower temperature, solution mixtures (PMH+*o*-TDH/*p*-TDH) ΔS_m^0 value decreased as the α_1 of hydrotrope increased. This implies that hydrotropes decreased the randomness at lower temperature, but at higher temperature, the ΔS_m^0 for the mixtures increased as the α_1 of hydrotrope increased. This indicates that at higher temperature, the presence of *o*-TDH/*p*-TDH increased the randomness of the system. The abrupt increase in ΔS_m^0 values at higher temperature occurred because a large amount of water was discharged from the tricyclic portion of PMH.

5. Mixed Micelle Formation in PMH and *o*-TDH/*p*-TDH Mixtures

As quantified above, the values of *cmc* and cmc^{id}, specify the attractive interaction in the solution mixtures. Consequently, the obtained values of *cmc* were employed to evaluate the constituent's composition in the mixed micelles formed. Rubingh [50] developed the first model based on a regular solution theory aimed at the nonideal mixing of solutions. This model is frequently used because of its simplicity. The constituent composition of mixed micelles is evaluated using Eq. (5) [50]:

$$\frac{(X_1^{Rb})^2 \ln[(\alpha_1 cmc/X_1^{Rb} cmc_1)]}{(1-X_1^{Rb})^2 \ln[(1-\alpha_1)cmc/(1-X_1^{Rb})cmc_2]} = 1 \quad (5)$$

X_1^{Rb} is the micellar composition of the first (*o*-TDH/*p*-TDH) component evaluated by Rubingh's model. Furthermore, the extent of interaction among constituents is called the interaction parameter (β), evaluated by applying Eq. (6) [51].

$$\beta = \frac{\ln[(cmc\,\alpha_1/cmc_1 X_1^{Rb})]}{(1-X_1^{Rb})^2} \quad (6)$$

For comparison purposes, experimentally evaluated *cmc* values were also analyzed via another model, suggested by Rodenas [52]. In this model, the constituent composition in mixed micelles is evaluated using Eq. (7) [52]:

$$X_1^{Rod} = -(1-\alpha_1)\alpha_1 \frac{d\ln cmc}{d\alpha_1} + \alpha_1 \quad (7)$$

The ideal mixed micelle composition of constituent 1 (X_1^{id}) was calculated using *cmc* values of the solution mixtures in Eq. (8) and this equation is derived from the Motomura model [53].

$$X_1^{id} = \frac{\alpha_1 cmc_2}{\alpha_1 cmc_2 + \alpha_2 cmc_1} \quad (8)$$

The micellar composition of constituent 1 computed via both models (X_1^{Rb} [Rubingh] and X_1^{Rod} [Rodenas]) along with X_1^{id} (ideal, Motomura) was always significantly greater than their corresponding bulk mole fraction (α_1) (Fig. 6 and Tables S1 and S2 (Supplementary Material)). All values of X_1^{Rb}, X_1^{Rod}, and X_1^{id} increased as the *o*-TDH/*p*-TDH concentration in the system increased, indicating that the mixed micelles experienced greater hydrotrope participation as expected from the α_1 value, and their participation in mixed micelles increased as α_1 increased [54,55]. At all α_1, the participation of hydrotropes in mixed micelles was determined by different models: $X_1^{Rod} > X_1^{Rb} > X_1^{id}$. Moreover, X_1^{Rb} and X_1^{Rod} values diverged from the X_1^{id} value representing the non-ideal conduct of the studied systems and in whole cases, the X_1^{Rb} and X_1^{Rod} values were greater than the X_1^{id} value, implying that *o*-TDH/*p*-TDH involvement in mixed micelles was higher than expected under ideal mixing. Fig. 6 and Tables S1 and S2 (Supplementary Material) show that although the employed mole fraction of both hydrotropes (*o*-TDH and *p*-TDH) in the solution mixtures was the same, the contribution in mixed micelles was greater for *p*-TDH than *o*-TDH. The lower tendency of *o*-TDH toward micellization is attributable to the presence of one methyl group at ortho location, creating a conformational hindrance that decreases its hydrophobicity. Consequently, it is concluded that the *p*-TDH hydrotrope integrates

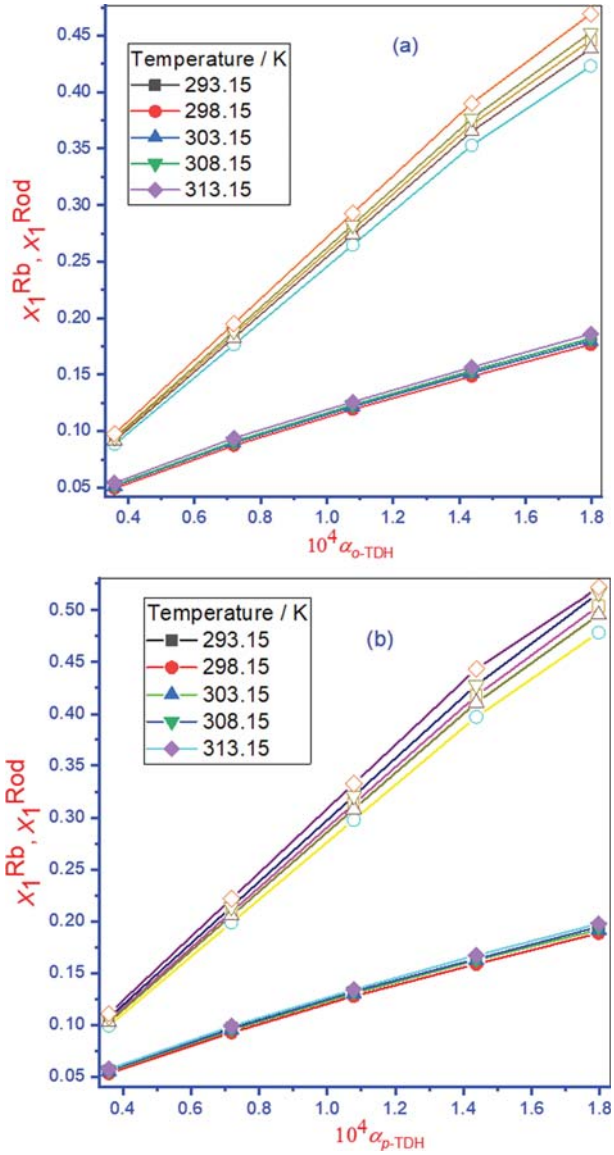

Fig. 6. Effect of α_1 of *o*-TDH/*p*-TDH and temperature on the X_1^{Rb} and X_1^{Rod} ((a) PMH–*o*-TDH, and (b) PMH–*o*-TDH mixtures, filled symbols, and open symbols represent the Rubingh and Rodenas models, respectively).

more easily into mixed micelles than *o*-TDH. The X_1^{id} values show maxima at 298.15 K; however, X_1^{Rb} and X_1^{Rod} values were lowest at 298.15 K. The utilized α_1 of *o*-TDH/*p*-TDH was very low in solution mixtures. Therefore, ideally in mixed micelles, their involvement must also remain minor; consequently, the X_1^{id} values were lower and close to the values of α_1. X_1^{Rb} and X_1^{Rod} values for *o*-TDH/*p*-TDH were much lower than the X_2^{Rb} and X_2^{Rod} of PMH in mixed micelles, implying that the TDH/*p*-TDH molecules only engaged with the formed PMH micelles.

The values of interaction parameter (β) among constituents using Eq. (6) are shown in Fig. 7. The values of β provide information regarding the type as well as the extent of interaction amid both employed constituents. In previous studies, there are three different β probabilities: negative, positive, or zero [2]. Negative β

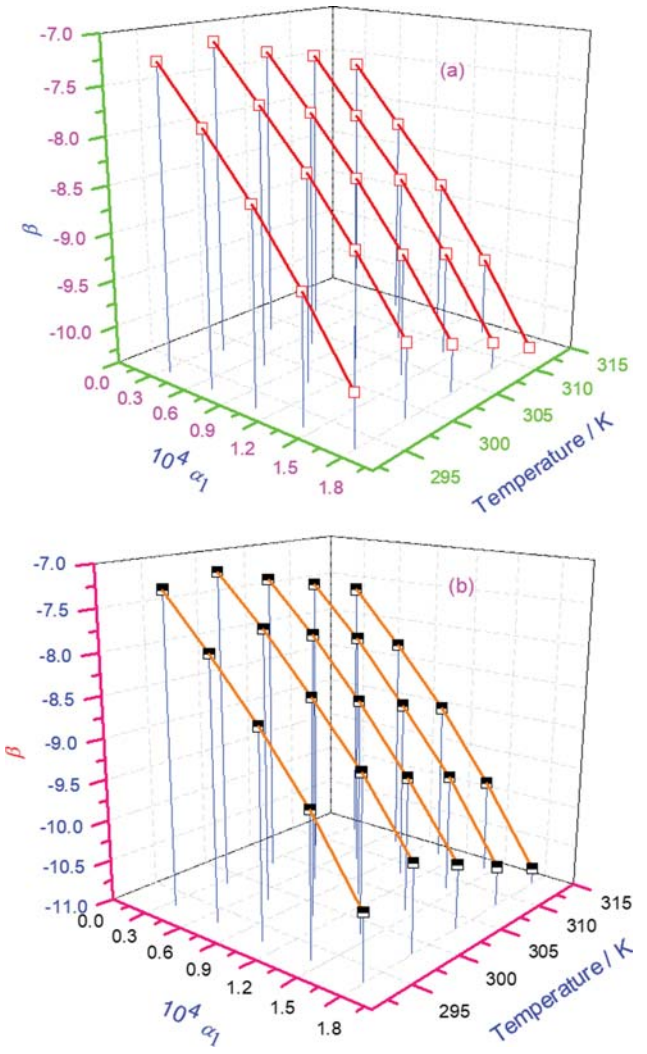

Fig. 7. Effect of the mole fraction of hydrotropes (α_1) and temperature on the variation of β in (a) PMH–*o*-TDH mixed systems, and (b) PMH–*p*-TDH mixed systems.

values indicate attractive or synergistic interaction between two constituents after mixing, positive β values indicate repulsive interaction among components, and β=zero or near zero specifies very little or no interaction through mixing, assuming ideal mixing. Steric effects contribute to the β value when the size of the head group portions of both mixture constituents is different or in the branching of the hydrophobic portions of both constituents [2].

The values of β in all our studied systems were negative, representing that the formed mixed micelles were as a result of the attractive or synergistic interactions among the studied constituents (Fig. 7). Higher negative values of β show a greater degree of interaction among constituents. Negative values of β increased with an increase in α_1 of *o*-TDH/*p*-TDH but varying temperature showed insignificant effects on the value, showing that interaction increased with an increase in α_1 of *o*-TDH/*p*-TDH. The average value of β (β_{av}) was –7 to –11. The β_{av} values for the PMH–*p*-TDH mixture were greater than the values for the PMH–*o*-TDH mixture, which was consistent for values of X_1^{Rb} and X_1^{Rod} in addition to their respective *cmc* value. This shows that *p*-TDH interactions were stronger than those of *o*-TDH. The aromatic counter ions were found to be more effective for penetrating the inner head group area, causing the diminishing of repulsion among them. This resulted in an increase in hydrophobic interaction among the components, causing micellar growth [56].

The occurrence of synergism or attractive interaction in any mixed system has been determined mathematically, if the system follows two conditions [2]: (i) β<0 and (ii) the absolute value of β must be higher than $|\ln(cmc_1/cmc_2)|$. The β values shown in Fig. 7 are negative. The value of β was much higher than $|\ln(cmc_1/cmc_2)|$, showing a large degree of synergism in the experimental systems (Fig. 7 and Tables S1 and S2 (Supplementary Material)).

6. Activity Coefficient

Another parameter, as part of the Rubingh model of mixed systems of both constituents, is the activity coefficient (f_1^{Rb} (*o*-TDH/*p*-TDH) and f_2^{Rb} (PMH)), determined using Eqs. (9) and (10).

$$f_1^{Rb} = \exp[\beta(1-X_1^{Rb})^2] \quad (9)$$

$$f_2^{Rb} = \exp[\beta(X_1^{Rb})^2] \quad (10)$$

Activity coefficients (f_1^{Rod} (o-TDH/p-TDH) and f_2^{Rod} (PMH)) were also evaluated by the Rodenas model, using Eqs. (11) and (12):

$$f_1^{Rod} = \frac{\alpha_1 cmc}{X_1^{Rod} cmc_1} \quad (11)$$

$$f_2^{Rod} = \frac{(1-\alpha_1) cmc}{(1-X_1^{Rod}) cmc_2} \quad (12)$$

The evaluated values of activity coefficients using both models are shown in Tables S1 and S2 (Supplementary Material). In all cases, the f_1 and f_2 value was below unity, demonstrating the existence of non-ideality in mixed systems (Tables S1 and S2 (Supplementary Material)). The value of f_1^{Rb} (*o*-TDH/*p*-TDH) and f_1^{Rod} (*o*-TDH/*p*-TDH) was much lower than the f_2^{Rb} (PMH) and f_2^{Rod} (PMH) values, confirming leading (maximum) participation of PMH in formed mixed micelles. Summation of activity coefficient values of PMH and *o*-TDH/*p*-TDH was also shown below one, demonstrating the existence of interaction between both components.

7. Excess Free Energy

The excess free energy (ΔG_{ex}) was determined by employing both current proposed models using Eqs. (13) and (14) as given below [57-61].

$$\Delta G_{ex}^{Rb} = RT[X_1^{Rb} \ln f_1^{Rb} + (1-X_1^{Rb}) \ln f_2^{Rb}] \quad (13)$$

$$\Delta G_{ex}^{Rod} = RT[X_1^{Rod} \ln f_1^{Rod} + (1-X_1^{Rod}) \ln f_2^{Rod}] \quad (14)$$

The ΔG_{ex}^{Rb} (Rubingh) and ΔG_{ex}^{Rod} (Rodenas) values in all cases of the entire composition range of the *o*-TDH/*p*-TDH were negative, as seen in Fig. 8. These values reveal the higher stability of mixed micelle formation than individual component micelle formation. The negative values of ΔG_{ex}^{Rb} (Rubingh) and ΔG_{ex}^{Rod} (Rodenas) occurred because of the increase in *o*-TDH/*p*-TDH mole fraction (α_1). This indicates that the stability of mixed systems increased through enhanced concentration of *o*-TDH/*p*-TDH in the solution mixtures, but their values were not notably changed

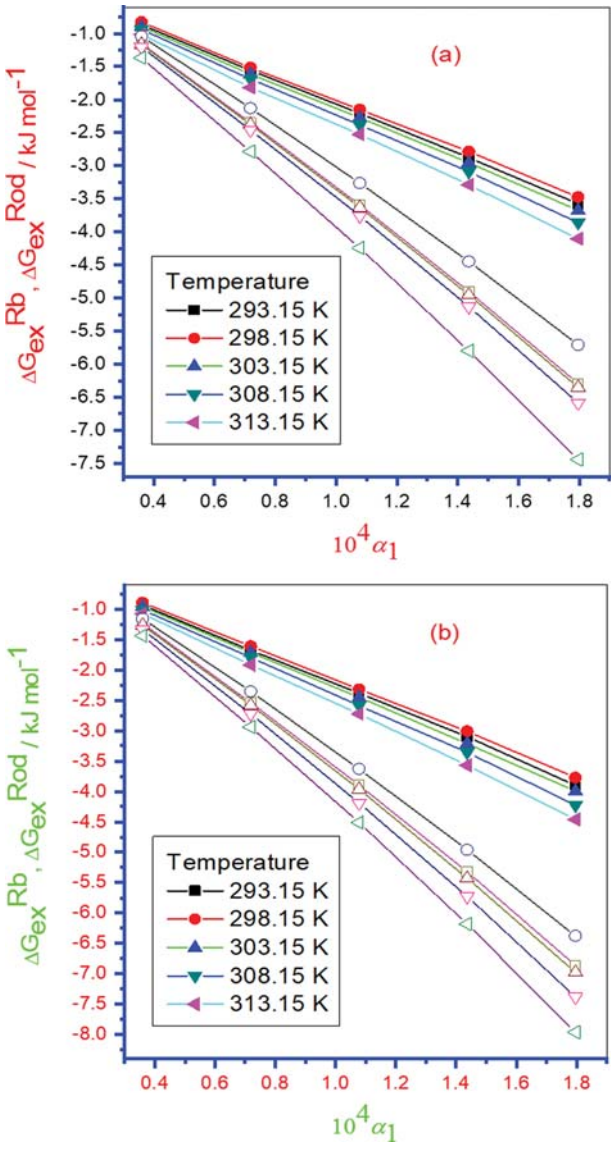

Fig. 8. The variation of ΔG_{ex}^{Rb} and ΔG_{ex}^{Rod} with hydrotrope mole fraction (α_1) in (a) PMH–*o*-TDH mixed systems, and (b) PMH–*p*-TDH mixed systems (filled symbols and open symbols represent the Rubingh and Rodenas models, respectively).

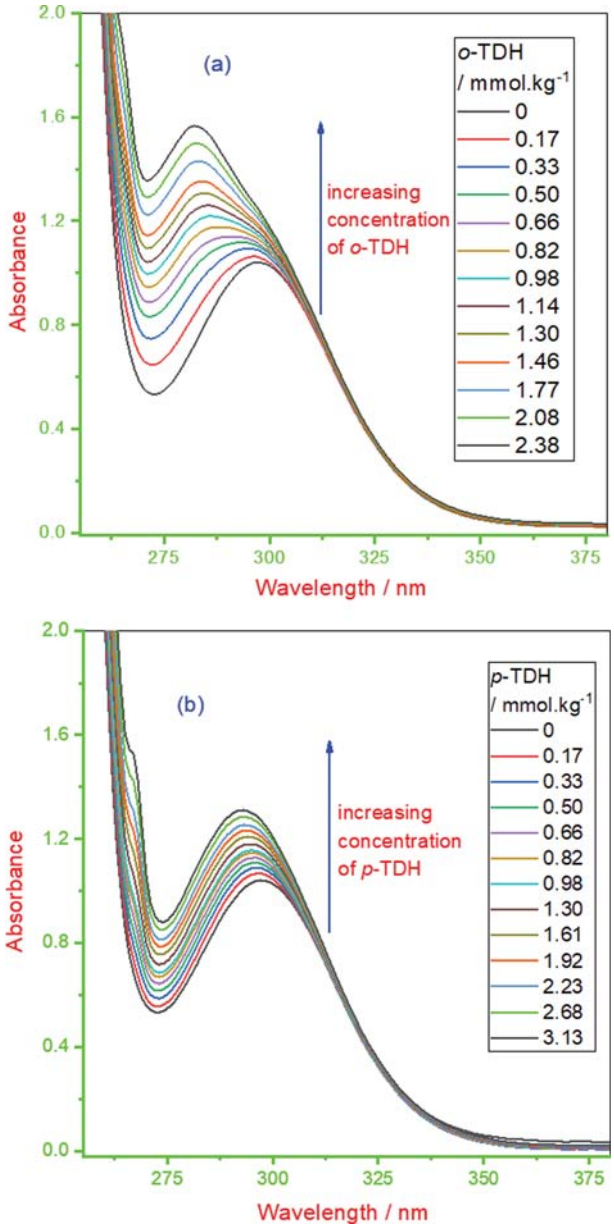

Fig. 9. UV-visible spectra of PMH in absence and presence of increasing concentration of (a) *p*-TDH and (b) *p*-TDH.

by temperature (Fig. 8). The ΔG_{ex} values were more negative for PMH–*p*-TDH mixtures than PMH–*o*-TDH mixtures, demonstrating that the mixed micelles formed through PMH and *p*-TDH mixtures displayed higher stability than PMH and *o*-TDH mixed systems and there were greater interactions in PMH and *p*-TDH mixtures. Fig. 8 also shows that the ΔG_{ex}^{Rb} and ΔG_{ex}^{Rod} values were in the same range at the lowest α_1 of hydrotropes; however, the ΔG_{ex}^{Rod} values were more negative than the ΔG_{ex}^{Rb} values.

8. UV-visible Study

The interactions of employed phenothiazine drug PMH with *o*-TDH/p-TDH (hydrotropes) have been more explored via the UV-visible spectroscopic method. The aromatic ring of PMH drug is accountable for its significant absorption characteristics, which change through its local atmosphere and consequently can be utilized to probe PMH–*o*-TDH/p-TDH interactions. In an aqueous medium, the absorption spectra of PMH drug in pure form and by the varying concentration of *o*-TDH/*p*-TDH (hydrotrope) are shown in Fig. 9. In the case of singular PMH (0.25 mmol·kg^{-1}), the wavelength (λ_{max}) of maximum absorption was detected at 297 nm and this obtained wavelength was chiefly because of n-π^* transition. Earlier literature [62] shows that the maximum absorption wavelength (λ_{max}) band was sustained by the existence of lone pairs of electrons on S-atom in the tricyclic ring of drug. As is clear from the figure that with the gradual addition of hydrotrope into the solution of PMH, a simultaneous increase in absorbance (hyperchromic effect) as well as blue shift, also called hypsochromic shift, takes place. The concentration of *o*-TDH was varied from 0.17 to 2.38 mmol·kg^{-1} while the concentration of *p*-TDH

was varied from 0.17 to 3.13 mmol·kg^{-1} into the solution of PMH. The obtained hyperchromism effect and hypsochromic shift confirm the interaction between PMH and *o*-TDH/*p*-TDH (hydrotrope) [63]. The shift in λ_{max} of PMH in the direction of shorter wavelength through increasing concentration of *o*-TDH/*p*-TDH is found low (about 5 nm) in magnitude in the presence of *p*-TDH while shifting in λ_{max} was found quite more (above 10 nm) in case of *o*-TDH.

9. FT-IR Measurement

Herein, FT-IR measurements of studied systems were also been employed to examine the interactions among the components of mixed micellar systems [64]. The headgroup as well as hydrophobic chain frequencies of amphiphiles give knowledge regarding the structural changes in the monomer of micelles [65]. In an aqueous system background-deducted FT-IR spectra of singular PMH and equal ratio of PMH+*o*-TDH mixtures are exposed in Fig. 10(a) and (b). The interaction of *o*-TDH with PMH possibly will occur owing to the shifting in the C-N stretching, and C-H stretching and bending frequency of the PMH head group. Fig. 10(a) shows a selected frequency region in between 1,025 to 1,470 cm^{-1} of singular PMH and PMH+*o*-TDH mixture to investigate the effect of *o*-TDH on aliphatic C-N stretching along with C-H bending in the PMH monomers head group. Employed drug PMH is cationic and that keeps N atom to whom three alkyl groups are attached directly. In the case of singular PMH drug spectra, the C-N stretching frequency was detected at four different wavenumbers (cm^{-1}) (1,061.67, 1,127.37, 1,144.41, and 1,175.56 cm^{-1}). In the presence of *o*-TDH in solution of PMH, i.e., PMH+*o*-TDH mixture, the C-N stretching frequencies in PMH were shifted from their original position (1,061.67 (PMH) to 1,062.36 cm^{-1} (PMH+*o*-TDH), 1,127.37 (PMH) to 1,126.77 cm^{-1} (PMH+*o*-TDH), 1,144.41 (PMH) to 1,145.02 cm^{-1} (PMH+*o*-TDH), and 1,175.56 (PMH) to 1,172.52

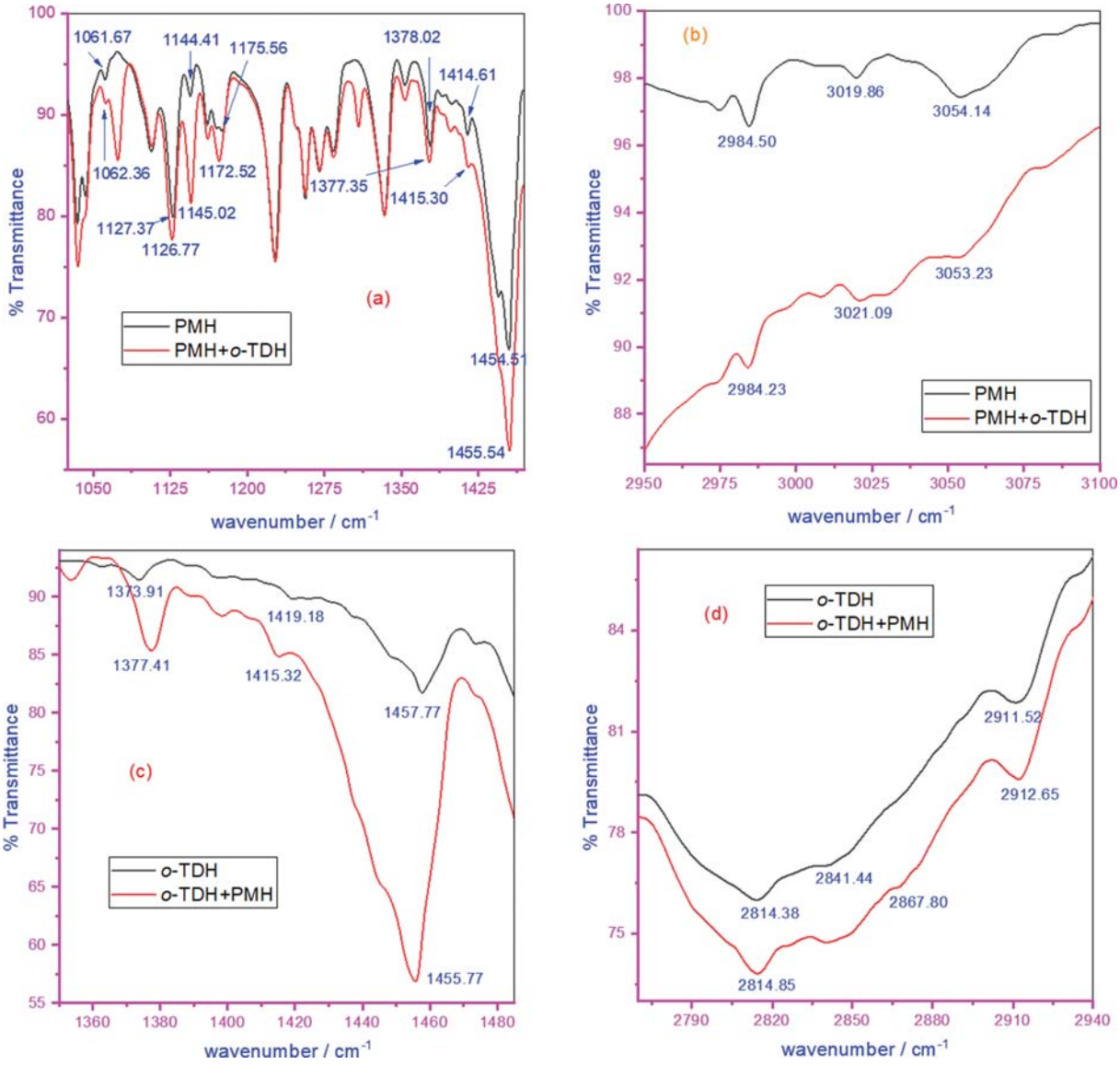

Fig. 10. FTIR spectra of PMH in absence and presence of *o*-TDH ((a) and (b)) and spectra of *o*-TDH in absence and presence of PMH ((c) and (d)) (mixtures are in equal ratio).

cm^{-1} PMH+*o*-TDH)). However, in case of pure PMH, the C-H bending was recorded at three different frequencies: first one at 1,378.02, the second at 1,414.61 and the third at 1,454.51 cm^{-1}. These obtained C-H bending frequencies in PMH were alerted in presence of *o*-TDH, which was found at 1,377.35, 1,415.30, and 1,455.54 cm^{-1} from their original position 1,378.02, 1,414.61, and 1,454.51 cm^{-1}, respectively. For the further investigation of PMH and *o*-TDH interaction, we chose another frequency region between 2,950-3,100 cm^{-1} to assess the consequence of *o*-TDH on C-H stretching of PMH and their plot is shown in Fig. 10(b). The C-H stretching in PMH was shown at three different wavenumbers (cm^{-1}): 2,984.50, 3,019.86, and 3,054.14 cm^{-1}, and in presence of *o*-TDH, their original value was moved to 2,884.23, 3,021.09, and 3,053.23, respectively. It is concluded from the shifting of C-N stretching, C-H stretching, and C-H bending frequency band in PMH drug, in presence of *o*-TDH specifies the clear interaction between both components [66].

Fig. 10(c) and (d) show the FT-IR spectra of singular *o*-TDH as well as the *o*-TDH+PMH mixed system in nearly identical ratios. A frequency range of 1,350 to 1,485 cm^{-1} was selected to investigate the effect of PMH drug on the C-H bending of the methyl group in *o*-TDH (Fig. 10(c)). The pure *o*-TDH showed C-H bending at 1,373.91, 1,419.18, and 1,457.77 cm^{-1} and in presence of PMH, these obtained C-H bending bands were shifted from their original position (1,373.91 to 1,377.41 cm^{-1}, 1,419.18 to 1,415.32 cm^{-1}, and 1,457.77 to 1,455.77 cm^{-1}), demonstrating an interaction among these constituents. Fig. 10(d) shows the spectra of the *o*-TDH and *o*-TDH+PMH mixed system in the frequency range of 2,770-2,940 cm^{-1} to assess the effect of PMH on N-H stretching of amine salt and C-H stretching band in *o*-TDH. The singular *o*-TDH revealed an N-H stretching of amine salt and a C-H stretching band at 2,814.38, 2,841.44, and 2,911.52 cm^{-1}. But, with the addition of PMH in the solution of *o*-TDH, endorsed a shifting in these bands toward a higher wavenumber (2,814.85, 2,867.80, and

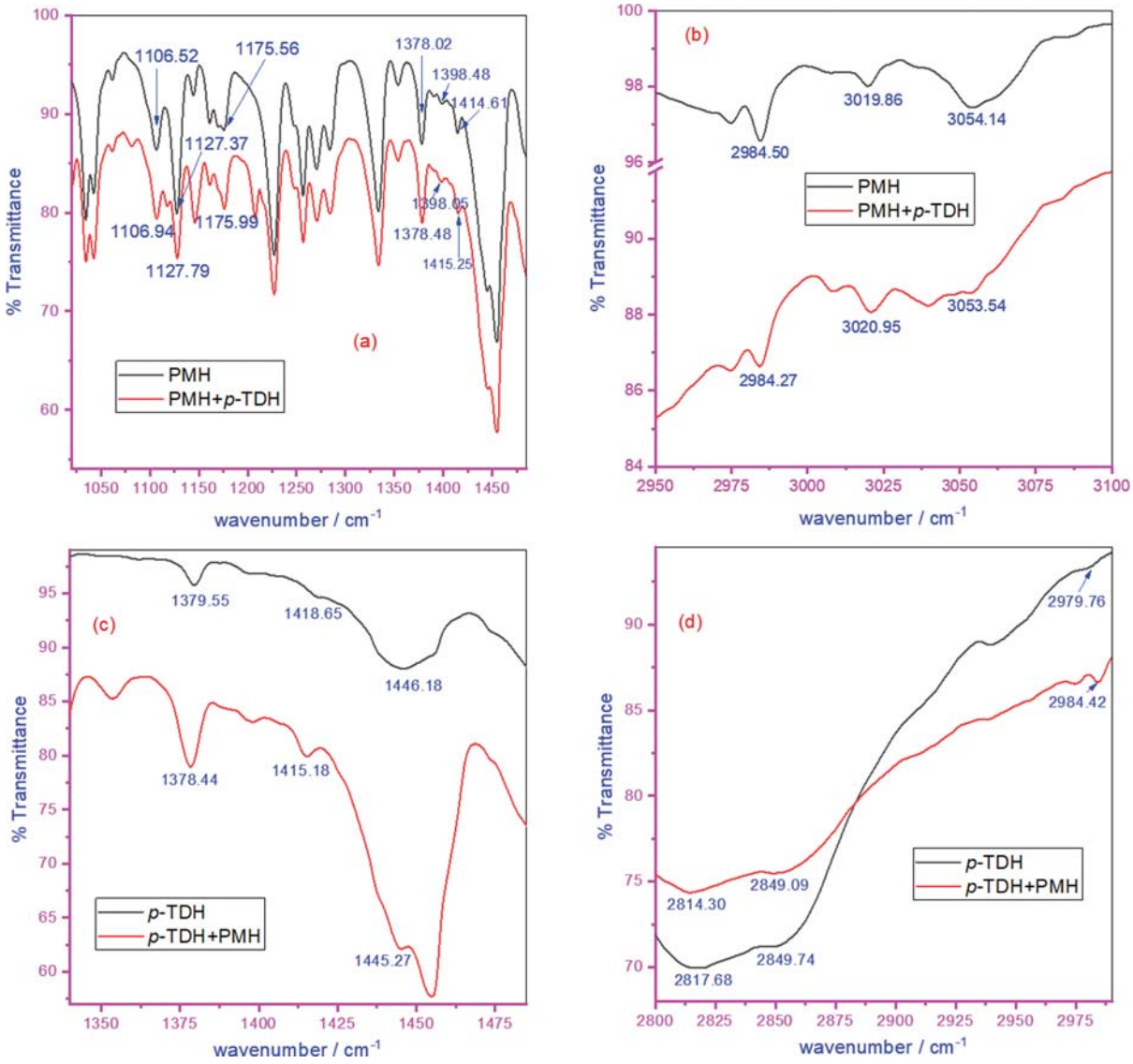

Fig. 11. FTIR spectra of PMH in absence and presence of *p*-TDH ((a) and (b)) and spectra of *p*-TDH in absence and presence of PMH ((c) and (d)) (mixtures are in equal ratio).

2,912.65 cm^{-1} respectively). This attained shifting of frequency in *o*-TDH in presence of PMH specified an interaction among employed constituents. Because of the interactions amid PMH and *o*-TDH, the frequency changes were detected; however, values are small but reproducible [64].

Fig. 11(a) and (b) show the FT-IR spectra of PMH in the absence and presence of *p*-TDH in an equal ratio. In Fig. 11(a) a frequency region 1,020-1,485 cm^{-1} was selected to view the effect of *p*-TDH on C-N stretching and C-H bending in the PMH molecules head group. In presence of *p*-TDH, the change in C-N stretching frequency in PMH spectra was sensed at three dissimilar wavenumbers (cm^{-1}). In PMH, the first C-N stretching was found at 1,106.52, the second at 1,127.37, and the third at 1,175.56 cm^{-1}); and in the presence of *p*-TDH these obtained frequencies were changed from their original position to higher frequency region (i.e., at 1,106.94, 1,127.79, and 1,175.99, respectively). The effect of *p*-TDH on C-H bending in PMH was detected at three different frequencies. In pure PMH, C-H bending was found at the following frequencies: 1,378.02, 1,398.48, and 1,414.61 cm^{-1}, and these values were shifted to 1,378.48, 1,398.05, and 1,415.25 cm^{-1}, respectively, in presence of *p*-TDH (Fig. 11(a)). The investigation of C-H stretching in PMH molecules in the absence and presence of *p*-TDH is shown in Fig. 11(b) and for this, we selected 2,950-3,100 cm^{-1} frequency region like for PMH and *o*-TDH mixtures. The *p*-TDH altered the C-H stretching in PMH at three diverse frequencies. In PMH, the C-H stretching was attained at 2,984.50, 3,019.86, and 3,054.14 cm^{-1}, and in the case of PMH+*p*-TDH, the attained C-H stretching frequency in PMH was shifted to somewhat at a different frequency such as 2,984.27, 3,020.95, and 3,053.54 cm^{-1} due to interaction between them.

FT-IR spectra of pure *p*-TDH and in equal ratio mixture of *p*-TDH+PMH are shown in Fig. 11(c) and (d). Fig. 11(c) shows the spectra in the frequency region between 1,340-1,485 cm^{-1} to investigate the effect of PMH drug on the C-H bending of the methyl group in *p*-TDH. The pure *p*-TDH showed C-H bending at 1,379.55, 1,418.65, and 1,446.18 cm^{-1}, which were shifted to the lower frequency at 1,378.44, 1,415.18, and 1,445.27 cm^{-1}, respectively, in presence of PMH owing to the interaction with each other. For the determination of the consequence of PMH drug on N-H stretching of amine salt as well as C-H stretching band in *p*-TDH, a frequency range between 2,800-2,990 cm^{-1} was selected, and their plot is shown in Fig. 11(d). The N-H stretching of amine salt and C-H stretching band in the case of singular *p*-TDH were found at 2,817.68, 2,849.79, and 2,979.76 cm^{-1}. In presence of PMH, C-H stretching of amine salt and C-H stretching band were located at a somewhat different position (2,817.68 to 2,814.30 cm^{-1}, 2,849.79 to 2,849.09 cm^{-1}, and 2,979.76 to 2,884.42 cm^{-1}) because of interaction between *p*-TDH and PMH. Overall, the shifting in C-H bending, C-H stretching, C-N stretching, and N-H stretching of amine salt frequencies depicts the interaction among the constituents [67].

CONCLUSIONS

The aggregation behavior of the phenothiazine drug PMH in the presence and absence of cationic hydrotropes *o*-TDH and *p*-TDH was analyzed thoroughly by the conductometric method. The values of *cmc* and cmc^{id} show that PMH and *o*-TDH/*p*-TDH form mixed micelles via attractive interactions and the interactions in PMH−*p*-TDH mixtures were greater than those of PMH−*o*-TDH. The values of X_1^{Rb} and X_1^{Rod} were higher than X_1^{id}, validating the higher contribution of *o*-TDH/*p*-TDH in mixed micelles, as expected under ideal conditions. Determined β values also indicated attractive interactions among constituents and their negative values were higher in PMH−*p*-TDH mixtures. The negative ΔG_m^o values obtained show the spontaneity in the system and the extent of spontaneity was greater in PMH−*p*-TDH mixed systems. The values of ΔH_m^o were negative in case of pure hydrotropes, but for singular PMH and PMH−*o*-TDH/*p*-TDH mixtures their values were only negative at lower temperature and found positive at higher temperature. For pure PMH and PMH−*o*-TDH/*p*-TDH mixtures, at a lower temperature, the ΔS_m^o values were a smaller magnitude while their values more or less doubled. All activity coefficient values were below unity, signifying the nonideality in the system. Excess free energy values in the mixed micelles were more stable as compared with the micelles of single constituents and their magnitudes increased through a rise in the *o*-TDH/*p*-TDH mole fraction. The study of UV-visible outcomes shows a clear-cut interaction between PMH and *o*-TDH/*p*-TDH as the absorption of PMH increases along with blue shifting which takes place with increasing concentration of *o*-TDH/*p*-TDH. The results of FT-IR study showed the changes in wavelength of PMH on addition of *o*-TDH/*p*-TDH or vice versa also confirmed the interaction between constituents.

ACKNOWLEDGEMENTS

This project was funded by the Deanship of Scientific Research (DSR), King Abdulaziz University, Jeddah, Saudi Arabia, under grant no. (KEP-73-130-38). The authors, therefore, acknowledge with thanks DSR for technical and financial support. This article is dedicated to Prof. Kabir-ud-Din on his 75th birth year.

SUPPORTING INFORMATION

Additional information as noted in the text. This information is available via the Internet at http://www.springer.com/chemistry/journal/11814.

REFERENCES

1. S. M. Shaban and D. H. Kim, *Korean J. Chem. Eng.*, **37**, 1008 (2020).
2. M. J. Rosen, *Surfactants and interfacial phenomenon*, 3rd Ed., Wiley, New Jersey (2004).
3. N. Tahmasebi and M. Khalildashti, *Korean J. Chem. Eng.*, **37**, 448 (2020).
4. B. Kim, Y. Choi, J. Choi, Y. Shin and S. Lee, *Korean J. Chem. Eng.*, **37**, 1 (2020).
5. D. Kumar and M. A. Rub, *J. Phys. Org. Chem.*, **32**, e3918 (2019).
6. D. Kumar and M. A. Rub, *J. Mol. Liq.*, **274**, 639 (2019).
7. T. K. Vo and J. Kim, *Korean J. Chem. Eng.*, **37**, 571 (2020).
8. G. H. Li and C. G. Cho, *Korean J. Chem. Eng.*, **25**, 1444 (2008).

9. P. Taboada, D. Attwood, J. M. Ruso, M. Garcia, F. Sarmiento and V. Mosquera, *J. Colloid Interface Sci.*, **248**, 158 (2002).
10. D. Kumar, S. Hidayathulla and M. A. Rub, *J. Mol. Liq.*, **271**, 254 (2018).
11. A. Srivastava, H. Uchiyama, Y. Wada, Y. Hatanaka, Y. Shirakawa, K. Kadota and Y. Tozuka, *J. Mol. Liq.*, **277**, 349 (2019).
12. M. A. Rub, N. Azum, F. Khan, A. G. Al-Sehemi and A. M. Asiri, *Korean J. Chem. Eng.*, **32**, 2142 (2015).
13. M. A. Rub, N. Azum, F. Khan and A. M. Asiri, *J. Chem. Thermodyn.*, **121**, 199 (2018).
14. M. H. Hatzopoulos, J. Eastoe, P. J. Dowding, S. E. Rogers, R. Heenan and R. Dyer, *Langmuir*, **27**, 12346 (2011).
15. D. Balasubramanian, V. Srinivas, V. G. Gaikar and M. M. Sharma, *J. Phys. Chem.*, **93**, 3865 (1989).
16. B. K. Roy and S. P. Moulik, *Curr. Sci.*, **85**, 1148 (2003).
17. V. Srinivas, G. A. Rodley, K. Ravikumar, W. T. Robinson and M. M. Turnbull, *Langmuir*, **13**, 3235 (1997).
18. K. M. Sachin, S. A. Karpe, M. Singh and A. Bhattara, *R. Soc. Open Sci.*, **6**, 181979 (2019).
19. S. Schreier, S. V. P. Malheiros and E. de Paula, *Biochim. Biophys. Acta*, **1508**, 210 (2000).
20. M. Jones and J. Leroux, *Eur. J. Pharm. Biopharm.*, **48**, 101 (1999).
21. V. P. Torchilin, *J. Controlled Rel.*, **73** 137 (2001).
22. B. G. Katzung, *Basic and clinical pharmacology*, 9th Ed., McGraw-Hill, New York (2004).
23. R. K. Mahajan, S. Mahajan, A. Bhadani and S. Singh, *Phys. Chem. Chem. Phys.*, **14**, 887 (2012).
24. D. Kumar and M. A. Rub, *J. Mol. Liq.*, **238**, 389 (2017).
25. Z. A. Khan, M. Kamil, O. Sulaiman, R. Hashim, M. N. M. Ibrahim, A. J. Khanam and Kabir-ud-Din, *J. Dispersion Sci. Technol.*, **32**, 1452 (2011).
26. I. A. Khan, A. J. Khanam, M. S. Sheikh and Kabir-ud-Din, *J. Phys. Chem. B*, **115**, 15251 (2011).
27. G. Landázuri, J. Alvarez, F. Carvajal, E. R. Macías, A. González-Álvarez, E. P. Schulz, M. Frechero, J. L. Rodríguez, R. Minardi, P. C. Schulz and J. F. A. Soltero, *J. Colloid Interface Sci.,* **370**, 86 (2012).
28. J. H. Clint, *J. Chem. Soc., Faraday Trans., 1*, **71**, 1327 (1975).
29. P. Jafari-Chashmi and A. Bagheri, *J. Mol. Liq.*, **269**, 816 (2018).
30. J. Mata, D. Varade and P. Bahadur, *Thermochim. Acta*, **428** 147 (2005).
31. J. L. Lopez-Fontan, V. Costa, J. M. Ruso, G. Prieto and F. Sarmiento, *J. Chem. Eng. Data*, **49**, 1008 (2004).
32. F. Khan, M. S. Sheikh, M. A. Rub, N. Azum and A. M. Asiri, *J. Mol. Liq.*, **222**, 1020 (2016).
33. S. Mahbub, M. A. Rub, M. A. Hoque and M. A. Khan, *J. Phys. Org. Chem.*, **31**, e3872 (2018).
34. S. Mahbub, M. A. Rub, M. A. Hoque and M. A. Khan, *J. Phys. Org. Chem.*, **32**, e3917 (2019).
35. T. Asakawa, H. Kitano, A. Ohta and S. Miyagishi, *J. Colloid Interface Sci.*, **242**, 284 (2001).
36. H. Iijima, T. Kato and A. Soderman, *Langmuir*, **16**, 318 (2000).
37. N. Gorski and J. Kalus, *Langmuir*, **17**, 4211 (2001).
38. S. A. Buckingham, C. J. Garve and G. G. Warr, *J. Phys. Chem.*, **97**, 10236 (1993).
39. K. M. Kale, E. L. Cussler and D. F. Evans, *J. Phys. Chem.*, **84**, 593 (1980).
40. Y. Wang, P. L. Dubin and H. Zhang, *Langmuir*, **17**, 1670 (2001).
41. F. Jalali, M. Shamsipur and N. Alizadeh, *J. Chem. Thermodyn.*, **32**, 755 (2000).
42. M. A. Rub, N. Azum, F. Khan and A. M. Asiri, *J. Phys. Org. Chem.*, **30**, e3676 (2017).
43. M. A. Rub, F. Khan, D. Kumar and A. M. Asiri, *Tenside Surf. Deterg.*, **52**, 236 (2015).
44. Z. A. Khan, *J. Mol. Liq.*, **281**, 333 (2019).
45. A. J. Khanam, M. S. Sheikh, I. A. Khan and Kabir-ud-Din, *J. Ind. Eng. Chem.*, **20**, 3453 (2014).
46. A. Malliaris, *J. Phys. Chem.*, **91**, 6511 (1987).
47. S. Chauhan and L. Pathania, *J. Mol. Liq.*, **272**, 953 (2018).
48. F. Khan, M. A. Rub, N. Azum and A. M. Asiri, *J. Phys. Org. Chem.*, **31**, e3812 (2018).
49. V. B. Wagle, P. S. Kothari and V. G. Gaikar, *J. Mol. Liq.*, **133**, 68 (2007).
50. D. N. Rubingh, Mixed Micelle Solution, in: K. L. Mittal Ed., Solution Chemistry of Surfactants, vol. 1, Plenum, New York (1979).
51. S. Das, S. Ghosh and B. Das, *J. Chem. Eng. Data*, **63**, 3784 (2018).
52. V. Rodenas, M. Valiente and M. S. Villafruela, *J. Phys. Chem. B*, **103**, 4549 (1999).
53. K. Motomura, M. Yamanaka and M. Aratono, *Colloid Polym. Sci.*, **262**, 948 (1984).
54. M. A. Rub, N. Azum, S. B. Khan, H. M. Marwani and A. M. Asiri, *J. Mol. Liq.*, **212**, 532 (2015).
55. F. Khan, M. A. Rub, N. Azum, D. Kumar and A. M. Asiri, *J. Solution Chem.*, **44**, 1937 (2015).
56. O. Singh, P. Singla, R. Kaur and R. K. Mahajan, *Colloids Surf. A*, **523**, 43 (2017).
57. M. A. Rub, N. Azum and A. M. Asiri, *J. Chem. Eng. Data*, **62**, 3216 (2017).
58. D. Kumar, N. Azum, M. A. Rub and A. M. Asiri, *J. Mol. Liq.*, **262**, 86 (2018).
59. D. Kumar, M. A. Rub, N. Azum and A. M. Asiri, *J. Phys. Org. Chem.*, **31**, e3730 (2018).
60. N. Azum, M. A. Rub, A. M. Asiri and H. A. Kashmery, *J. Mol. Liq.*, **260**, 159 (2018).
61. M. A. Rub, F. Khan, M. S. Sheikh, N. Azum and A. M. Asiri, *J. Chem. Thermodyn.*, **96**, 196 (2016).
62. J.-J. Aaron, M. Maafi, C. Kersebet, C. Párkányi, M. S. Antonious and N. Motohashi, *J. Photochem. Photobiol. A*, **101**, 127 (1996).
63. S. Mahajan and R. K. Mahajan, *J. Colloid Interface Sci.*, **387**, 194 (2012).
64. H. Kumar, N. Sharma and A. Katal, *J. Mol. Liq.*, **258**, 285 (2018).
65. V. G. Gaikar, K. V. Padalkar and V. K. Aswal, *J. Mol. Liq.*, **138**, 155 (2008).
66. A. Nabi, S. Tasneem, C. G. Jesudason, V. S. Lee and S. B. M. Zain, *J. Mol. Liq.*, **256**, 100 (2018).
67. K. V. Padalkar, V. G. Gaikar and V. K. Aswal, *J. Mol. Liq.*, **144**, 40 (2009).

Supporting Information

Effect of low levels of hydrotropes on micellization of phenothiazine drug

Sulaiman Y. M. Alfaifi*, Dileep Kumar,***,†, Malik Abdul Rub*,****, Farah Khan*****, Naved Azum*,****, Anish Khan*,****, Abdullah M. Asiri*,****, and Hurija Džudžević-Čančar******

*Chemistry Department, Faculty of Science, King Abdulaziz University, Jeddah-21589, Saudi Arabia
**Division of Computational Physics, Institute for Computational Science, Ton Duc Thang University, Ho Chi Minh City, Vietnam
***Faculty of Applied Sciences, Ton Duc Thang University, Ho Chi Minh City, Vietnam
****Center of Excellence for Advanced Materials Research, King Abdulaziz University, Jeddah-21589, Saudi Arabia
*****Department of Chemistry, Aligarh Muslim University, Aligarh-202 002, India
******Department of Natural Science in Pharmacy, Faculty of Pharmacy, University of Sarajevo, Zmaja od Bosne 8, 71 000 Sarajevo, Bosnia and Herzegovina
(*Received 23 June 2020 • Revised 16 October 2020 • Accepted 11 November 2020*)

Table S1. Physico-chemical parameters for aqueous PMH – *o*-TDH mixtures at different temperatures and composition[a]

α_1	cmc/mmol·kg^{-1}	cmc^{id}/mmol·kg^{-1}	g	ΔG^{o}_{m}/kJ·mol^{-1}	$10^4.X_1^{id}$	f_1^{Rb}/f_1^{Rod}	f_2^{Rb}/f_2^{Rod}	$\ln(cmc_1/cmc_2)$
		T=293.15 K						
0	36.51		0.65	−24.11				
0.36×10^{-4}	33.95	36.50	0.64	−24.53	0.84	0.0015/0.0011	0.981/0.999	
0.72×10^{-4}	31.20	36.49	0.63	−24.99	1.68	0.0016/0.0010	0.939/0.993	
1.08×10^{-4}	28.20	36.49	0.61	−25.70	2.52	0.0016/0.0009	0.881/0.976	−0.85
1.44×10^{-4}	25.0	36.48	0.59	−26.48	3.36	0.0015/0.0008	0.808/0.948	
1.80×10^{-4}	21.60	36.47	0.58	−27.17	4.20	0.0014/0.0007	0.722/0.907	
1	15.62		0.59	−28.10				
		T=298.15 K						
0	38.31		0.69	−23.64				
0.36×10^{-4}	35.80	38.30	0.67	−24.22	0.85	0.0016/0.0013	0.983/0.997	
0.72×10^{-4}	33.0	38.29	0.66	−24.67	1.69	0.0017/0.0012	0.943/0.985	
1.08×10^{-4}	30.01	38.29	0.65	−25.18	2.54	0.0017/0.0011	0.889/0.964	−0.86
1.44×10^{-4}	26.85	38.28	0.63	−25.93	3.39	0.0016/0.0009	0.822/0.935	
1.80×10^{-4}	23.40	38.28	0.62	−26.59	4.23	0.0015/0.0008	0.740/0.889	
1	16.25		0.66	−27.03				
		T=303.15 K						
0	37.01		0.70	−23.96				
0.36×10^{-4}	34.45	37.00	0.69	−24.38	0.78	0.0014/0.0011	0.981/0.998	
0.72×10^{-4}	31.65	36.99	0.67	−25.04	1.55	0.0015/0.0010	0.939/0.988	
1.08×10^{-4}	28.70	36.98	0.66	−25.56	2.33	0.0015/0.0009	0.883/0.972	−0.77
1.44×10^{-4}	25.50	36.98	0.64	−26.35	3.10	0.0014/0.0008	0.812/0.943	
1.80×10^{-4}	22.10	36.97	0.63	−27.03	3.88	0.0013/0.0007	0.727/0.899	
1	17.15		0.67	−27.09				
		T=308.15 K						
0	36.05		0.72	−24.07				
0.36×10^{-4}	33.50	36.04	0.71	−24.50	0.72	0.0013/0.0010	0.980/0.996	
0.72×10^{-4}	30.70	36.03	0.70	−24.98	1.43	0.0013/0.0009	0.936/0.984	
1.08×10^{-4}	27.75	36.03	0.68	−25.71	2.15	0.0013/0.0008	0.878/0.965	−0.69
1.44×10^{-4}	24.55	36.02	0.67	−26.32	2.86	0.0013/0.0007	0.804/0.932	
1.80×10^{-4}	21.15	36.02	0.66	−27.03	3.58	0.0012/0.0006	0.715/0.885	
1	18.10		0.71	−26.53				

Table S1. Continued

α_1	cmc/mmol·kg^{-1}	cmc^{id}/mmol·kg^{-1}	g	ΔG_m^o/kJ·mol^{-1}	$10^4.X_1^{id}$	f_1^{Rb}/f_1^{Rod}	f_2^{Rb}/f_2^{Rod}	$\ln(cmc_1/cmc_2)$
		T=313.15 K						
0	34.75		0.73	−24.39				
0.36×10^{-4}	32.15	34.74	0.72	−24.84	0.66	0.0011/0.0008	0.978/0.999	
0.72×10^{-4}	29.3	34.73	0.70	−25.54	1.31	0.0012/0.0008	0.930/0.989	
1.08×10^{-4}	26.45	34.73	0.69	−26.09	1.97	0.0012/0.0007	0.869/0.977	−0.60
1.44×10^{-4}	23.20	34.72	0.68	−26.74	2.62	0.0011/0.0006	0.791/0.946	
1.80×10^{-4}	19.80	34.71	0.67	−27.49	3.28	0.0010/0.0005	0.698/0.901	
1	19.05		0.73	−26.38				

[a]Relative standard uncertainties (u_r) limits are $u_r(cmc/cmc^{id})=\pm3\%$, $u_r(g)=\pm3\%$, $u_r(\Delta G_m^o)=\pm3\%$, $u_r(X_1^{id})=2\%$, $u_r(f_1^{Rb}/f_1^{Rod})=\pm4\%$ and $u_r(f_2^{Rb}/f_2^{Rod})=\pm4\%$.

Table S2. Physico-chemical parameters for aqueous PMH−*p*-TDH mixtures at different temperatures and composition[a]

α_1	cmc/mmol·kg^{-1}	cmc^{id}/mmol·kg^{-1}	g	ΔG_m^o/kJ·mol^{-1}	$10^4.X_1^{id}$	f_1^{Rb}/f_1^{Rod}	f_2^{Rb}/f_2^{Rod}	$\ln(cmc_1/cmc_2)$
		T=293.15 K						
0.36×10^{-4}	33.70	36.49	0.63	−24.73	0.94	0.0015/0.0012	0.978/0.998	
0.72×10^{-4}	30.65	36.48	0.62	−25.23	1.87	0.0016/0.0010	0.929/0.988	
1.08×10^{-4}	27.35	36.48	0.6	−25.99	2.81	0.0016/0.0009	0.862/0.967	−0.96
1.44×10^{-4}	23.85	36.47	0.58	−26.83	3.74	0.0015/0.0008	0.799/0.934	
1.80×10^{-4}	20.05	36.47	0.56	−27.82	4.68	0.0013/0.0007	0.679/0.879	
1	14.01		0.75	−25.24				
		T=298.15 K						
0.36×10^{-4}	35.55	38.29	0.66	−24.43	0.94	0.0016/0.0013	0.979/0.997	
0.72×10^{-4}	32.55	38.28	0.65	−24.90	1.89	0.0017/0.0012	0.936/0.987	
1.08×10^{-4}	29.15	38.28	0.64	−25.46	2.83	0.0017/0.0010	0.872/0.961	−0.96
1.44×10^{-4}	25.65	38.27	0.62	−26.27	3.77	0.0016/0.0009	0.795/0.927	
1.80×10^{-4}	21.9	38.27	0.6	−27.20	4.71	0.0014/0.0008	0.702/0.876	
1	14.60		0.77	−25.13				
		T=303.15 K						
0.36×10^{-4}	34.2	36.99	0.68	−24.59	0.86	0.0014/0.0011	0.978/0.997	
0.72×10^{-4}	31.2	36.98	0.66	−25.28	1.73	0.0015/0.0010	0.931/0.988	
1.08×10^{-4}	27.85	36.97	0.64	−26.04	2.59	0.0015/0.0009	0.865/0.964	−0.88
1.44×10^{-4}	24.25	36.97	0.63	−26.71	3.45	0.0014/0.0008	0.781/0.926	
1.80×10^{-4}	20.55	36.96	0.62	−27.48	4.32	0.0013/0.0007	0.687/0.876	
1	15.40		0.78	−25.18				
		T=308.15 K						
0.36×10^{-4}	33.25	36.03	0.7	−24.71	0.78	0.0013/0.0010	0.977/0.997	
0.72×10^{-4}	30.25	36.02	0.68	−25.41	1.56	0.0014/0.0009	0.928/0.986	
1.08×10^{-4}	26.85	36.02	0.66	−26.21	2.34	0.0013/0.0008	0.857/0.959	−0.78
1.44×10^{-4}	23.35	36.01	0.64	−27.09	3.12	0.0012/0.0007	0.774/0.923	
1.80×10^{-4}	19.55	36.01	0.63	−27.91	3.90	0.0011/0.0006	0.671/0.865	
1	16.60		0.8	−24.95				
		T=313.15 K						
0.36×10^{-4}	31.95	34.73	0.71	−25.06	0.71	0.0011/0.0008	0.975/0.997	
0.72×10^{-4}	28.9	34.72	0.69	−25.79	1.42	0.0012/0.0008	0.923/0.985	
1.08×10^{-4}	25.6	34.72	0.67	−26.6	2.13	0.0012/0.0007	0.852/0.960	−0.68
1.44×10^{-4}	22	34.71	0.65	−27.53	2.85	0.0011/0.0006	0.759/0.918	
1.80×10^{-4}	18.3	34.71	0.64	−28.39	3.56	0.0009/0.0005	0.656/0.861	
1	17.55		0.81	−24.97	0.71			

[a]Relative standard uncertainties (u_r) limits are $u_r(cmc/cmc^{id})=\pm3\%$, $u_r(g)=\pm3\%$, $u_r(\Delta G_m^o)=\pm3\%$, $u_r(X_1^{id})=2\%$, $u_r(f_1^{Rb}/f_1^{Rod})=\pm4\%$ and $u_r(f_2^{Rb}/f_2^{Rod})=\pm4\%$.

Table S3. Concentration-specific conductivity (κ) data of pure drug promethazine hydrochloride (PMH) in aqueous media at different temperatures

Temp=293.15 K		Temp=298.15 K		Temp=303.15 K		Temp=308.15 K		Temp=313.15 K	
Conc/ mmol·kg^{-1}	κ/ mS cm^{-1}	Conc/ mmol·kg^{-1}	κ/ mS cm^{-1}	Conc/ mmol·kg^{-1}	κ/ mS cm^{-1}	Conc/ mmol·kg^{-1}	κ/ mS cm^{-1}	Conc/ mmol·kg^{-1}	κ/ mS cm^{-1}
0	0	0	0	0	0	0	0	0	0
3.2653	0.2376	3.2653	0.2277	3.2653	0.2376	3.2653	0.2376	3.2425	0.24069
6.4	0.4455	6.4	0.4158	6.4	0.4356	6.4	0.4356	6.3552	0.44126
9.4118	0.6435	9.4118	0.6138	9.4118	0.6336	9.4118	0.6435	9.3459	0.65187
12.308	0.8217	12.308	0.7722	12.308	0.8118	12.308	0.8217	12.222	0.83238
15.094	0.99	15.094	0.9306	15.094	0.9801	15.094	0.99	14.989	1.00287
17.778	1.1484	17.778	1.0989	17.778	1.1484	17.778	1.1583	17.653	1.17336
20.364	1.2969	20.364	1.2474	20.364	1.2969	20.364	1.3068	20.221	1.32379
22.857	1.4355	22.857	1.3761	22.857	1.4454	22.857	1.4454	22.697	1.46419
25.263	1.5642	25.263	1.5048	25.263	1.5741	25.263	1.5741	25.086	1.59456
27.586	1.6929	27.586	1.6236	27.586	1.7028	27.586	1.7127	27.393	1.73497
29.831	1.8117	29.831	1.7424	29.831	1.8216	29.831	1.8315	29.622	1.85531
32	1.9206	32	1.8513	32	1.9305	32	1.9503	31.776	1.97565
34.098	2.0295	34.098	1.9503	34.098	2.0295	34.098	2.0592	33.86	2.08597
36.129	2.1285	36.129	2.0493	36.129	2.1285	36.129	2.1681	35.876	2.19629
38.095	2.2275	38.095	2.1483	38.095	2.2275	38.095	2.2671	37.829	2.29657
40	2.3265	40	2.2473	40	2.3265	40	2.376	39.72	2.40689
41.846	2.4156	41.846	2.3265	41.846	2.4156	41.846	2.475	41.553	2.50718
43.636	2.5047	43.636	2.4057	43.636	2.5047	43.636	2.5641	43.331	2.59743
45.373	2.5839	45.373	2.475	45.373	2.574	45.373	2.6532	45.056	2.68769
47.059	2.6532	47.059	2.5443	47.059	2.6433	47.059	2.7423	46.729	2.77795
48.696	2.7225	48.696	2.6136	48.696	2.7126	48.696	2.8215	48.355	2.85818
50.286	2.7819	50.286	2.6829	50.286	2.772	50.286	2.9007	49.934	2.93841
51.831	2.8413	51.831	2.7423	51.831	2.8413	51.831	2.97	51.468	3.00861
53.333	2.9007	53.333	2.8017	53.333	2.9106	53.333	3.0393	52.96	3.07881
54.795	2.9601	54.795	2.8611	54.795	2.97	54.795	3.1086	54.411	3.14901
56.216	3.0195	56.216	2.9205	56.216	3.0294	56.216	3.1779	55.823	3.21921
57.6	3.0789	57.6	2.97	57.6	3.0888	57.6	3.2373	57.197	3.27938
58.947	3.1383	58.947	3.0195	58.947	3.1383	58.947	3.2967	58.535	3.33956
60.26	3.1878	60.26	3.069	60.26	3.1878	60.26	3.3462	59.838	3.3897
61.538	3.2373	61.538	3.1185	61.538	3.2373	61.538	3.3957	61.108	3.43984
62.785	3.2868	62.785	3.168	62.785	3.2868	62.785	3.4452	62.345	3.48999
64	3.3363	64	3.2175	64	3.3363	64	3.4947	63.552	3.54013
65.185	3.3759	65.185	3.2571	65.185	3.3759	65.185	3.5343	64.729	3.58025
		66.341	3.2967	66.341	3.4155	66.341	3.5739	65.877	3.62036
		67.47	3.3363	67.47	3.4551				
		68.571	3.3759	68.571	3.4947				

Table S4. Concentration-specific conductivity (κ) data of pure ortho-toluidine hydrochloride (*o*-TDH) in aqueous media at different temperatures

Temp=293.15 K		Temp=298.15 K		Temp=303.15 K		Temp=308.15 K		Temp=313.15 K	
Conc/ mmol·kg^{-1}	κ/ mS cm^{-1}	Conc/ mmol·kg^{-1}	κ/ mS cm^{-1}	Conc/ mmol·kg^{-1}	κ/ mS cm^{-1}	Conc/ mmol·kg^{-1}	κ/ mS cm^{-1}	Conc/ mmol·kg^{-1}	κ/ mS cm^{-1}
0	0	0	0	0	0	0	0	0	0
1.4852	0.2528	1.4852	0.1782	1.4852	0.21342	1.4852	0.13205	1.4823	0.13456
2.9412	0.4794	2.9412	0.342	2.9412	0.39367	2.9412	0.26389	2.9356	0.2689
4.3689	0.6751	4.3689	0.5057	4.3689	0.56362	4.3689	0.38852	4.3606	0.3959
5.7692	0.8646	5.7692	0.6623	5.7692	0.72327	5.7692	0.5183	5.7583	0.52815
7.1429	1.0428	7.1429	0.8044	7.1429	0.87674	7.1429	0.64705	7.1293	0.65934
8.4906	1.1932	8.4906	0.9219	8.4906	1.01476	8.4906	0.76653	8.4744	0.78109
9.8131	1.3374	9.8131	1.0331	9.8131	1.1569	9.8131	0.86335	9.7944	0.87975
11.111	1.4919	11.111	1.1876	11.111	1.2805	11.111	0.95605	11.09	0.97421
12.385	1.6258	12.385	1.3524	12.385	1.4041	12.385	1.04875	12.362	1.06868
13.636	1.7597	13.636	1.476	13.636	1.538	13.636	1.15175	13.61	1.17363
14.865	1.8936	14.865	1.5687	14.865	1.6822	14.865	1.24445	14.837	1.26809
16.071	2.0275	16.071	1.6408	16.071	1.8058	16.071	1.33715	16.041	1.36256
17.257	2.1511	17.257	1.7129	17.257	1.9294	17.257	1.42985	17.224	1.45702
18.421	2.2747	18.421	1.8159	18.421	2.0427	18.421	1.52255	18.386	1.55148
19.565	2.3777	19.565	1.9086	19.565	2.1457	19.565	1.62555	19.528	1.65644
20.69	2.4807	20.69	2.0013	20.69	2.2487	20.69	1.71825	20.65	1.7509
21.795	2.5837	21.795	2.0837	21.795	2.3517	21.795	1.80065	21.753	1.83486
22.881	2.6867	22.881	2.1661	22.881	2.4547	22.881	1.88305	22.838	1.91883
23.95	2.7794	23.95	2.2485	23.95	2.5474	23.95	1.95515	23.904	1.9923
25	2.8721	25	2.3309	25	2.6401	25	2.02725	24.953	2.06577
26.033	2.9545	26.033	2.4133	26.033	2.7225	26.033	2.08905	25.984	2.12874
27.049	3.0369	27.049	2.4854	27.049	2.7946	27.049	2.15085	26.998	2.19172
28.049	3.109	28.049	2.5575	28.049	2.8667	28.049	2.21265	27.995	2.25469
29.032	3.1811	29.032	2.6296	29.032	2.9285	29.032	2.26415	28.977	2.30717
30	3.2429	30	2.6914	30	2.9903	30	2.31565	29.943	2.35965
30.952	3.3047	30.952	2.7429	30.952	3.0521	30.952	2.36715	30.894	2.41213
31.89	3.3562	31.89	2.7944	31.89	3.1036	31.89	2.40835	31.829	2.45411

Table S5. Concentration-specific conductivity (κ) data of pure para-toluidine hydrochloride (*p*-TDH) in aqueous media at different temperatures

Temp=293.15 K		Temp=298.15 K		Temp=303.15 K		Temp=308.15 K		Temp=313.15 K	
Conc/ mmol·kg^{-1}	κ/ mS cm^{-1}	Conc/ mmol·kg^{-1}	κ/ mS cm^{-1}	Conc/ mmol·kg^{-1}	κ/ mS cm^{-1}	Conc/ mmol·kg^{-1}	κ/ mS cm^{-1}	Conc/ mmol·kg^{-1}	κ/ mS cm^{-1}
0	0	0	0	0	0	0	0	0	0
1.4852	0.15077	1.5876	0.14765	1.4852	0.14863	1.4852	0.19838	1.4739	0.20267
2.9412	0.2857	3.0262	0.28156	2.9412	0.28459	2.9412	0.36421	2.9188	0.37208
4.3689	0.41548	4.3714	0.40659	4.3689	0.42776	4.3689	0.51562	4.3357	0.52676
5.7692	0.52363	5.7166	0.51308	5.7692	0.55548	5.7692	0.64849	5.7254	0.6625
7.1429	0.64723	7.1429	0.64399	7.1429	0.67702	7.1429	0.78136	7.0886	0.79824
8.4906	0.75126	8.1921	0.74943	8.4906	0.78311	8.4906	0.90187	8.426	0.92135
9.8131	0.85323	9.8131	0.84896	9.8131	0.89229	9.8131	1.01929	9.7385	1.04131
11.111	0.94902	11.111	0.94427	11.111	1.00044	11.111	1.11714	11.027	1.14127
12.385	1.03863	12.385	1.03344	12.385	1.09932	12.385	1.23044	12.291	1.25702
13.636	1.12103	13.461	1.12373	13.636	1.19202	13.636	1.34374	13.533	1.37276
14.865	1.20343	14.544	1.20843	14.865	1.28472	14.865	1.46734	14.752	1.49903
16.071	1.28583	15.833	1.29798	16.071	1.37742	16.071	1.58064	15.949	1.61478
17.257	1.34763	16.861	1.36896	17.257	1.45982	17.257	1.67334	17.125	1.70948
18.421	1.44033	18.103	1.45851	18.421	1.55252	18.421	1.76604	18.281	1.80419
19.565	1.52273	19.393	1.53433	19.565	1.64522	19.565	1.85874	19.417	1.89889
20.69	1.60513	20.532	1.61419	20.69	1.72762	20.69	1.96174	20.532	2.00411
21.795	1.68753	21.513	1.70293	21.795	1.79972	21.795	2.06474	21.629	2.10934
23.239	1.79053	22.952	1.79247	23.239	1.91302	23.239	2.18834	23.063	2.23561
24.652	1.89353	24.652	1.88406	24.652	2.02632	24.652	2.30164	24.464	2.35136
26.033	1.98623	25.894	1.98849	26.033	2.12932	26.033	2.41494	25.835	2.4671
27.384	2.06863	27.137	2.05948	27.384	2.22202	27.384	2.51794	27.176	2.57233
28.706	2.15103	28.706	2.14027	28.706	2.31472	28.706	2.61064	28.488	2.66703
30	2.23343	30	2.22226	30	2.38682	30	2.69304	29.772	2.75121
31.266	2.31583	31.107	2.29181	31.266	2.46922	31.266	2.77544	31.029	2.83539
32.507	2.38793	32.452	2.34989	32.507	2.54132	32.507	2.84754	32.259	2.90905
33.721	2.46003	33.592	2.42571	33.721	2.61342	33.721	2.91964	33.465	2.9827
34.91	2.53213	34.881	2.48783	34.91	2.68552	34.91	2.98144	34.645	3.04584

Table S6. Concentration-specific conductivity (κ) data of promethazine hydrochloride (PMH) in the presence of *o*-TDH (α_1)=0.36×10^{-4} in aqueous media at different temperatures

Temp=293.15 K		Temp=298.15 K		Temp=303.15 K		Temp=308.15 K		Temp=313.15 K	
Conc/ mmol·kg^{-1}	κ/ mS cm^{-1}	Conc/ mmol·kg^{-1}	κ/ mS cm^{-1}	Conc/ mmol·kg^{-1}	κ/ mS cm^{-1}	Conc/ mmol·kg^{-1}	κ/ mS cm^{-1}	Conc/ mmol·kg^{-1}	κ/ mS cm^{-1}
0	0	0	0	0	0	0	0	0	0
3.4905	0.2334	3.2078	0.20788	3.1212	0.20788	3.2359	0.23712	3.1777	0.23876
6.5966	0.429	6.6537	0.41764	6.4632	0.42953	6.3424	0.43473	6.2281	0.43773
9.4327	0.62459	9.4416	0.59712	9.632	0.61442	9.3271	0.64221	9.159	0.64666
12.303	0.80563	12.308	0.78224	12.299	0.81121	12.197	0.82006	11.978	0.82572
15.24	1.0033	15.094	0.9427	14.777	0.97128	14.958	0.98802	14.689	0.99485
17.778	1.16459	17.778	1.11319	17.405	1.13806	17.618	1.15598	17.3	1.16397
20.169	1.31751	20.364	1.26362	19.936	1.28523	20.062	1.3439	19.817	1.3132
22.701	1.47357	22.636	1.41562	22.377	1.43239	22.473	1.46978	22.243	1.45248
25.267	1.61299	24.939	1.53455	24.732	1.55993	25.036	1.57095	24.584	1.5818
27.631	1.74616	27.586	1.64471	27.007	1.68747	27.338	1.70927	26.845	1.72109
29.893	1.87101	29.831	1.76505	29.205	1.80521	29.563	1.82784	29.03	1.84047
32	1.94768	32	1.87537	31.328	1.91313	31.712	1.9464	31.14	1.95984
34.098	2.05812	34.098	1.97565	33.382	2.01123	33.791	2.05508	33.183	2.06928
36.129	2.15851	36.129	2.07594	35.37	2.10934	35.804	2.16376	35.158	2.17872
38.095	2.25891	38.095	2.17623	37.295	2.20745	37.752	2.26257	37.072	2.2782
40	2.3593	40	2.27651	39.16	2.30556	39.64	2.37125	38.926	2.38763
41.541	2.44532	41.846	2.35674	40.967	2.39386	41.469	2.47005	40.722	2.48712
43.466	2.55352	43.636	2.43697	42.72	2.48216	43.243	2.55897	42.464	2.57665
45.373	2.62033	45.373	2.50718	44.42	2.55083	44.965	2.64789	44.155	2.66619
47.059	2.69061	47.059	2.57738	45.892	2.62227	46.635	2.73682	45.794	2.75573
48.696	2.76089	48.576	2.66985	47.329	2.69363	48.258	2.81586	47.388	2.83531
50.252	2.81155	50.286	2.71778	48.957	2.765	49.833	2.8949	48.935	2.9149
51.94	2.87397	51.727	2.78878	50.584	2.83095	51.365	2.96406	50.439	2.98454
53.459	2.93431	53.333	2.83812	52.212	2.89691	52.853	3.03322	51.901	3.05418
54.945	2.99258	54.602	2.90231	53.736	2.96286	54.302	3.10238	53.323	3.12382
56.397	3.03836	55.848	2.96286	55.035	3.00214	55.71	3.17154	54.707	3.19346
57.882	3.09038	57.6	3.00861	56.39	3.061	57.188	3.22396	56.053	3.25314
59.402	3.14656	58.947	3.05875	57.709	3.11006	58.773	3.29671	57.364	3.31284
60.988	3.19858	60.26	3.1089	58.995	3.15911	59.718	3.33951	58.641	3.36258
62.17	3.24436	61.538	3.15904	60.246	3.20816	60.984	3.38891	59.886	3.41232
63.521	3.30262	62.785	3.20918	61.467	3.25722	62.316	3.42952	61.098	3.46207
64.837	3.34216	64	3.25933	62.656	3.30627	63.61	3.48264	62.281	3.51181
66.289	3.39418	65.185	3.29944	63.816	3.34552			63.434	3.55161
		66.341	3.33956	64.948	3.38476				
		67.47	3.37967						
		68.571	3.41979						

Table S7. Concentration-specific conductivity (κ) data of promethazine hydrochloride (PMH) in the presence of *o*-TDH (α_1)=0.72×10^{-4} in aqueous media at different temperatures

Temp=293.15 K		Temp=298.15 K		Temp=303.15 K		Temp=308.15 K		Temp=313.15 K	
Conc/ mmol·kg^{-1}	κ/ mS cm^{-1}	Conc/ mmol·kg^{-1}	κ/ mS cm^{-1}	Conc/ mmol·kg^{-1}	κ/ mS cm^{-1}	Conc/ mmol·kg^{-1}	κ/ mS cm^{-1}	Conc/ mmol·kg^{-1}	κ/ mS cm^{-1}
0	0	0	0	0	0	0	0	0	0
3.3822	0.21939	3.1597	0.207693	3.09312	0.2083	3.3839	0.23221	3.2707	0.22137
6.7541	0.43891	6.5539	0.417264	6.40503	0.43039	6.2472	0.41975	6.0376	0.39699
9.6876	0.63182	9.2999	0.596583	9.54534	0.61565	9.1105	0.62789	8.8797	0.61489
12.52	0.81364	12.123	0.781536	12.188	0.81283	11.965	0.81268	11.618	0.81334
15.116	0.97773	14.868	0.941852	14.644	0.97322	14.497	0.99864	14.249	0.97992
17.78	1.17064	17.511	1.112188	17.248	1.14034	16.972	1.14499	16.781	1.14651
20.364	1.34544	20.059	1.262483	19.7569	1.2878	19.681	1.3318	19.09	1.30652
22.857	1.48922	22.297	1.414346	22.1756	1.43525	22.046	1.45655	21.256	1.44419
25.263	1.62274	24.565	1.533169	24.5099	1.56305	24.56	1.55681	23.511	1.60572
27.586	1.75626	27.172	1.64323	26.7636	1.69084	26.818	1.69389	25.752	1.70545
29.831	1.8795	29.384	1.763461	28.9417	1.80882	29.001	1.81139	27.917	1.84313
32	1.99248	31.52	1.873682	31.046	1.91696	31.109	1.92888	30.206	1.93045
34.098	2.10545	33.587	1.973872	33.0815	2.01525	33.149	2.03658	32.187	2.03824
36.129	2.20816	35.587	2.074072	35.052	2.11356	35.124	2.14429	34.104	2.14604
38.095	2.31086	37.524	2.174271	36.9594	2.21186	37.035	2.24221	35.96	2.24402
40.405	2.39463	39.4	2.274461	38.8076	2.31017	38.887	2.34991	37.758	2.35182
42.732	2.47667	41.218	2.354619	40.5985	2.39865	40.681	2.44782	39.5	2.44982
44.856	2.54984	42.981	2.434777	42.3352	2.48712	42.483	2.55102	40.729	2.54777
46.677	2.62523	44.692	2.504924	44.0204	2.55593	43.955	2.6345	42.624	2.62257
48.531	2.68732	46.353	2.57506	45.4787	2.62751	45.749	2.71219	44.421	2.71439
50.352	2.76936	47.847	2.667447	46.903	2.69902	47.433	2.7841	45.966	2.79278
52.206	2.83588	49.532	2.715334	48.5161	2.77053	49.1	2.85456	47.556	2.87733
54.23	2.89353	50.951	2.78627	50.1292	2.83661	50.523	2.91202	49.12	2.94671
55.814	2.96005	52.533	2.835566	51.7422	2.9027	52.011	2.97273	50.414	3.015
57.163	3.00884	53.783	2.899698	53.2523	2.96879	53.726	3.03669	51.707	3.05837
58.478	3.06427	55.011	2.960193	54.5401	3.00814	54.826	3.10715	53.18	3.13317
59.827	3.11971	56.736	3.005902	55.8829	3.06712	56.298	3.16461	54.308	3.17111
60.906	3.14853	58.063	3.055997	57.1897	3.11628	57.544	3.2058	55.602	3.2329
61.85	3.17514	59.356	3.106102	58.4636	3.16543	58.87	3.26976	57.241	3.29578
62.828	3.21283	60.615	3.156197	59.7035	3.21458	60.213	3.33047	58.368	3.36407
64.008	3.27492	61.843	3.206292	60.9133	3.26373	61.491	3.36841	59.265	3.41014
65.424	3.3237	63.04	3.256397	62.0921	3.31288				
66.874	3.3747	64.207	3.296471	63.2418	3.35221				
				64.3633	3.39153				

Table S8. Concentration-specific conductivity (κ) data of promethazine hydrochloride (PMH) in the presence of *o*-TDH (α_1)=1.08×10^{-4} in aqueous media at different temperatures

Temp=293.15 K		Temp=298.15 K		Temp=303.15 K		Temp=308.15 K		Temp=313.15 K	
Conc/ mmol·kg^{-1}	κ/ mS cm^{-1}	Conc/ mmol·kg^{-1}	κ/ mS cm^{-1}	Conc/ mmol·kg^{-1}	κ/ mS cm^{-1}	Conc/ mmol·kg^{-1}	κ/ mS cm^{-1}	Conc/ mmol·kg^{-1}	κ/ mS cm^{-1}
0	0	0	0	0	0	0	0	0	0
3.2417	0.23048	3.206	0.18668	3.0034	0.20455	3.2824	0.22989	3.1863	0.2196
6.1374	0.44334	6.1502	0.39048	6.2193	0.42264	6.0598	0.41555	5.8818	0.39381
8.7184	0.64734	9.1232	0.59479	9.2685	0.60457	9.015	0.62323	8.8045	0.60838
11.677	0.85134	11.893	0.77919	11.835	0.7982	11.607	0.80455	11.391	0.77641
14.258	1.03981	14.585	0.93903	14.219	0.9557	14.158	0.97282	13.391	0.95095
16.744	1.22607	17.179	1.10885	16.748	1.11981	16.463	1.13354	16.348	1.13734
18.938	1.38714	19.677	1.2587	19.184	1.26462	19.075	1.29809	18.598	1.29607
21.277	1.55646	21.873	1.4101	21.533	1.40942	21.384	1.44198	20.707	1.43264
23.386	1.6895	24.099	1.52857	23.799	1.53491	23.602	1.56662	22.905	1.59287
25.655	1.8107	26.656	1.6383	25.987	1.66041	25.767	1.68619	25.087	1.69181
27.742	1.93777	28.825	1.75817	28.102	1.77626	28.131	1.79328	27.197	1.82838
29.76	2.05424	30.921	1.86806	30.146	1.88245	30.176	1.90959	29.427	1.91501
31.711	2.17072	32.948	1.96795	32.122	1.97898	32.155	2.01621	31.357	2.02193
33.6	2.27661	34.911	2.06785	34.035	2.07551	33.602	2.12799	33.224	2.12887
35.429	2.3825	36.811	2.16775	35.888	2.17205	35.737	2.23236	35.032	2.22607
37.549	2.47002	38.651	2.26764	37.682	2.26859	37.72	2.32641	36.784	2.33301
39.406	2.54319	40.396	2.36131	39.421	2.35547	39.316	2.44414	38.481	2.43022
41.075	2.62967	42.165	2.42747	41.107	2.44236	41.209	2.52551	40.459	2.50983
42.554	2.69619	43.697	2.51091	42.744	2.50992	42.637	2.60816	41.932	2.59114
44.033	2.77823	45.472	2.56734	44.16	2.58022	44.368	2.67112	43.662	2.65293
45.607	2.82923	47.094	2.64317	45.543	2.65043	46.01	2.75626	45.226	2.73423
46.992	2.89575	48.591	2.70719	47.109	2.72066	47.627	2.82601	46.955	2.80903
48.503	2.96005	50.232	2.76892	48.675	2.78555	49.165	2.86871	48.248	2.87733
50.139	3.02658	51.535	2.82706	50.242	2.85046	50.451	2.943	49.376	2.9337
51.619	3.0931	52.82	2.87624	51.708	2.91535	52.114	3.00632	50.94	2.98357
52.878	3.15297	54.341	2.93587	52.958	2.954	53.286	3.05921	52.233	3.04644
54.514	3.21505	55.861	2.99658	54.262	3.01191	54.338	3.10481	53.361	3.11474
55.994	3.29044	56.96	3.04683	55.531	3.06019	55.818	3.17374	54.744	3.17111
57.158	3.33479	58.228	3.09678	56.768	3.10845	57.316	3.23249	56.383	3.23941
58.323	3.39688	59.463	3.14673	57.972	3.15671				
59.676	3.45009	60.682	3.18845	59.147	3.20499				
60.841	3.49444	61.847	3.22423	60.291	3.25325				
62.005	3.54544	63.093	3.27735	61.408	3.29187				
				62.497	3.33048				

Table S9. Concentration-specific conductivity (κ) data of promethazine hydrochloride (PMH) in the presence of *o*-TDH (α_1)=1.44×10^{-4} in aqueous media at different temperatures

Temp=293.15 K		Temp=298.15 K		Temp=303.15 K		Temp=308.15 K		Temp=313.15 K	
Conc/ mmol·kg^{-1}	κ/ mS cm^{-1}	Conc/ mmol·kg^{-1}	κ/ mS cm^{-1}	Conc/ mmol·kg^{-1}	κ/ mS cm^{-1}	Conc/ mmol·kg^{-1}	κ/ mS cm^{-1}	Conc/ mmol·kg^{-1}	κ/ mS cm^{-1}
0	0	0	0	0	0	0	0	0	0
3.069	0.25765	3.1483	0.185747	2.9493	0.20332	3.1872	0.22644	3.0907	0.21631
5.9586	0.4784	6.0394	0.388528	6.1074	0.4201	5.8841	0.40932	5.7054	0.3879
8.8481	0.71324	8.959	0.591816	9.1017	0.60094	8.7536	0.61388	8.5404	0.59925
11.446	0.90656	11.679	0.775294	11.622	0.79341	11.27	0.79248	11.049	0.76476
13.528	1.09604	14.323	0.934335	13.963	0.94997	13.747	0.95823	12.989	0.93669
16.323	1.30035	16.869	1.103306	16.447	1.11309	15.986	1.11654	15.858	1.12028
18.993	1.453	19.323	1.252407	18.669	1.27985	18.522	1.27862	18.04	1.27663
21.097	1.6033	21.479	1.40305	21.256	1.39638	21.071	1.42374	20.627	1.42147
23.495	1.72574	23.665	1.520927	23.371	1.5257	23.03	1.52507	22.349	1.54117
25.655	1.86774	26.176	1.630109	25.519	1.65045	25.02	1.6609	24.978	1.69386
27.742	1.99881	28.306	1.749379	27.596	1.7656	27.315	1.76638	26.866	1.77681
29.76	2.11895	30.365	1.85872	29.603	1.87116	29.301	1.88095	28.589	1.87672
31.711	2.2391	32.355	1.95811	31.544	1.96711	31.105	2.00031	30.502	1.96343
33.6	2.34832	34.283	2.057511	33.887	2.06111	32.815	2.08036	32.544	2.05768
35.429	2.45755	36.148	2.156911	35.707	2.14825	34.788	2.18473	34.496	2.15194
37.555	2.54738	37.956	2.256302	37.271	2.22425	36.748	2.27796	36.257	2.23771
39.346	2.63662	39.669	2.349503	39.511	2.30025	38.722	2.36713	38.069	2.32442
41.136	2.72351	41.406	2.415333	41.241	2.38131	40.389	2.44515	39.982	2.41585
42.832	2.80571	42.91	2.498355	43.06	2.45731	41.877	2.51304	41.679	2.48748
44.245	2.88555	44.654	2.554503	44.534	2.52115	43.461	2.59107	43.134	2.56006
45.878	2.93957	46.246	2.629954	46.429	2.586	45.143	2.67416	44.793	2.62981
47.198	3.01002	47.716	2.693654	48.083	2.66706	46.616	2.74914	46.298	2.70427
48.705	3.08517	49.328	2.755075	49.03	2.7076	48.006	2.81501	47.651	2.77402
50.087	3.14858	50.607	2.812925	50.158	2.75421	49.368	2.88087	48.812	2.8268
51.752	3.22373	51.869	2.861859	51.195	2.79575	50.674	2.93458	50.164	2.88806
52.914	3.28949	53.363	2.921191	52.233	2.85351	51.786	2.9822	51.453	2.94367
54.139	3.35994	54.856	2.981597	53.436	2.90012	52.842	3.04503		
55.552	3.4163	55.934	3.031596	54.82	2.94167				
56.714	3.47501	57.18	3.081296	56.203	3.01159				
57.814	3.52198	58.393	3.130996	57.331	3.06327				
58.976	3.56895	59.59	3.172508	58.895	3.12812				
60.232	3.62766								
61.488	3.68637								

Table S10. Concentration-specific conductivity (κ) data of promethazine hydrochloride (PMH) in the presence of *o*-TDH (α_1)=1.80×10^{-4} in aqueous media at different temperatures

Temp=293.15 K		Temp=298.15 K		Temp=303.15 K		Temp=308.15 K		Temp=313.15 K	
Conc/ mmol·kg^{-1}	κ/ mS cm^{-1}	Conc/ mmol·kg^{-1}	κ/ mS cm^{-1}	Conc/ mmol·kg^{-1}	κ/ mS cm^{-1}	Conc/ mmol·kg^{-1}	κ/ mS cm^{-1}	Conc/ mmol·kg^{-1}	κ/ mS cm^{-1}
0	0	0	0	0	0	0	0	0	0
3.0068	0.26234	3.0538	0.18296	2.8933	0.2021	3.0597	0.2235	3.032	0.2135
6.0714	0.49014	5.8583	0.3827	5.9913	0.41758	5.6487	0.404	5.5455	0.41106
8.4028	0.72025	8.6903	0.58294	8.9287	0.59733	8.4035	0.6059	8.2121	0.59957
11.062	0.91051	11.329	0.76366	11.401	0.78865	10.819	0.78218	10.547	0.77206
13.31	1.09604	13.893	0.92032	13.698	0.94427	13.197	0.94577	12.742	0.92451
15.872	1.28537	16.363	1.08676	16.134	1.10641	15.346	1.10202	15.434	1.12174
17.98	1.47179	18.744	1.23362	18.314	1.27217	17.781	1.262	17.697	1.26003
20.407	1.60672	20.835	1.382	20.852	1.388	20.228	1.40523	20.235	1.40299
22.555	1.75077	22.955	1.49811	22.927	1.51655	22.109	1.50524	21.925	1.52113
24.78	1.89216	25.391	1.60566	25.034	1.64055	24.019	1.63931	24.503	1.67184
26.882	2.04246	27.457	1.72314	27.072	1.75501	26.222	1.74342	26.356	1.75371
29.217	2.15284	29.454	1.83084	29.041	1.85993	28.129	1.8565	28.142	1.83807
31.435	2.27026	31.241	1.89999	30.925	1.93892	30.018	1.95966	30.132	1.9295
33.128	2.37125	33.662	1.97295	32.843	2.01433	31.829	2.02375	32.008	2.01621
34.85	2.45814	35.241	2.05098	34.524	2.08502	33.59	2.12743	33.858	2.10481
36.543	2.54503	37.226	2.129	36.442	2.17173	35.364	2.20755	35.657	2.17456
38.294	2.62488	39.06	2.20196	38.207	2.25279	37.239	2.29332	37.469	2.27447
39.549	2.71177	40.639	2.26884	40.445	2.3395	38.923	2.37721	39.23	2.36307
41.388	2.79162	41.962	2.33673	42.043	2.42151	40.659	2.45732	41.003	2.43564
42.935	2.85972	43.376	2.39753	44.045	2.49691	42.049	2.5299	42.534	2.50162
44.394	2.93957	44.955	2.45427	45.546	2.57048	43.517	2.59022	44.04	2.5742
45.62	3.01472	46.368	2.51	47.158	2.63829	44.984	2.6628	45.469	2.64112
47.108	3.09457	47.692	2.56573	48.284	2.68165	46.451	2.7316	46.974	2.71558
48.48	3.15797	49.195	2.63869	49.479	2.725	47.995	2.79852	48.289	2.77684
49.939	3.23078	50.774	2.70557	50.674	2.78438	49.233	2.85696		
51.253	3.30593	52.098	2.75624	51.717	2.82774				
52.566	3.37403	53.602	2.8069						
53.967	3.44918	54.925	2.86871						
55.427	3.51729	56.008	2.91836						
56.653	3.60418	57.752	2.98626						
57.966	3.6488								
59.133	3.70986								
60.272	3.77092								

Table S11. Concentration-specific conductivity (κ) data of promethazine hydrochloride (PMH) in the presence of *p*-TDH (α_1)=0.36×10^{-4} in aqueous media at different temperatures

Temp=293.15 K		Temp=298.15 K		Temp=303.15 K		Temp=308.15 K		Temp=313.15 K	
Conc/ mmol·kg^{-1}	κ/ mS cm^{-1}	Conc/ mmol·kg^{-1}	κ/ mS cm^{-1}	Conc/ mmol·kg^{-1}	κ/ mS cm^{-1}	Conc/ mmol·kg^{-1}	κ/ mS cm^{-1}	Conc/ mmol·kg^{-1}	κ/ mS cm^{-1}
0	0	0	0	0	0	0	0	0	0
3.2653	0.24057	3.71	0.22137	3.2033	0.235937	3.2	0.235699	3.3839	0.22372
6.4	0.45107	6.7056	0.38398	6.2784	0.432551	6.272	0.432115	6.2345	0.43817
9.4118	0.65154	9.4935	0.56502	9.233	0.629165	9.2236	0.638352	9.4664	0.63253
12.308	0.83197	12.576	0.74606	12.074	0.806117	12.062	0.815126	11.99	0.82655
15.094	1.00238	15.069	0.90758	14.807	0.973239	14.792	0.98208	14.704	0.99585
17.778	1.16276	17.753	1.07561	17.44	1.140361	17.422	1.149034	17.318	1.16515
20.364	1.31311	20.143	1.23172	19.977	1.287822	19.957	1.296346	19.658	1.34621
22.857	1.45344	22.491	1.36647	22.423	1.435282	22.4	1.433837	22.343	1.4744
25.263	1.58375	24.859	1.49427	24.783	1.563081	24.758	1.561507	24.478	1.62106
27.586	1.71406	27.145	1.61223	27.062	1.69088	27.034	1.698998	26.355	1.73539
29.831	1.83435	29.354	1.7302	29.264	1.808849	29.234	1.816848	29.04	1.8832
32	1.94461	31.488	1.83834	31.392	1.916987	31.36	1.934698	31.192	2.00331
34.098	2.05487	33.552	1.93665	33.45	2.015294	33.416	2.042726	33.149	2.09916
36.129	2.15511	35.551	2.03495	35.443	2.113601	35.406	2.150755	34.767	2.19501
38.095	2.25534	37.485	2.13326	37.371	2.211908	37.333	2.248963	37.177	2.29086
40	2.35558	39.36	2.23157	39.24	2.310215	39.2	2.356992	39.054	2.39364
41.846	2.4458	41.176	2.31021	41.051	2.398691	41.009	2.4552	40.763	2.48963
43.636	2.53601	42.938	2.38886	42.807	2.487167	42.763	2.543587	42.508	2.57925
45.373	2.6162	44.647	2.45768	44.511	2.555982	44.466	2.631974	44.2	2.66888
47.059	2.68637	46.306	2.52649	46.165	2.624797	46.118	2.720362	45.841	2.7585
48.696	2.75653	47.917	2.5953	47.771	2.693612	47.722	2.798928	47.436	2.83817
50.286	2.81667	49.481	2.66412	49.331	2.752596	49.28	2.877494	48.985	2.91784
51.831	2.87682	51.002	2.7231	50.846	2.821411	50.794	2.94624	50.232	2.99877
53.333	2.93696	52.48	2.78209	52.32	2.890226	52.266	3.014986	51.954	3.05726
54.795	2.9971	53.918	2.84107	53.754	2.94921	53.699	3.083731	53.377	3.12697
56.216	3.05724	55.317	2.90006	55.148	3.008194	55.092	3.152477	54.762	3.19668
57.6	3.11739	56.678	2.94921	56.506	3.067178	56.448	3.211402	56.039	3.24128
58.947	3.17753	58.004	2.99836	57.827	3.116332	57.768	3.270326	57.641	3.29902
60.26	3.22765	59.296	3.04752	59.115	3.165485	59.055	3.31943	58.903	3.35676
61.538	3.27777	60.553	3.09667	60.369	3.214639	60.307	3.368534	60.148	3.4145
62.785	3.32789	61.78	3.14582	61.592	3.263792	61.529	3.417638	61.16	3.46556
64	3.378	62.976	3.19498	62.784	3.312946	62.72	3.466742	62.345	3.51535
65.185	3.4181	64.142	3.2343	63.946	3.352269	63.881	3.506026	63.499	3.55519
		65.28	3.27362	65.081	3.391592	65.014	3.545309		
		66.39	3.31295						

Table S12. Concentration-specific conductivity (κ) data of promethazine hydrochloride (PMH) in the presence of *p*-TDH (α_1)=0.72×10^{-4} in aqueous media at different temperatures

Temp=293.15 K		Temp=298.15 K		Temp=303.15 K		Temp=308.15 K		Temp=313.15 K	
Conc/ mmol·kg^{-1}	κ/ mS cm^{-1}	Conc/ mmol·kg^{-1}	κ/ mS cm^{-1}	Conc/ mmol·kg^{-1}	κ/ mS cm^{-1}	Conc/ mmol·kg^{-1}	κ/ mS cm^{-1}	Conc/ mmol·kg^{-1}	κ/ mS cm^{-1}
0	0	0	0	0	0	0	0	0	0
3.2653	0.24382	3.6283	0.21827	3.6751	0.22787	3.303	0.23642	3.3264	0.22081
6.6537	0.45008	6.5581	0.3786	6.7487	0.44035	6.1466	0.42909	6.3233	0.43276
9.5281	0.64635	9.2847	0.55711	9.1752	0.60838	9.1105	0.60597	9.3055	0.62431
12.308	0.8432	12.299	0.73562	11.833	0.79967	11.821	0.80942	11.786	0.8158
15.094	1.01591	14.738	0.89487	14.511	0.96545	14.496	0.97521	14.454	0.9829
17.778	1.17845	17.264	1.04679	17.091	1.13124	17.074	1.14099	17.03	1.16342
20.16	1.36134	19.7	1.21448	19.578	1.27752	19.205	1.28962	19.324	1.32871
22.636	1.4929	21.996	1.34734	21.974	1.4238	21.793	1.46169	21.436	1.48105
25.026	1.64172	24.312	1.47335	24.287	1.55058	24.123	1.56332	23.857	1.6068
27.586	1.7372	26.547	1.58966	26.521	1.67735	26.494	1.68711	25.907	1.71283
29.831	1.85911	28.708	1.70598	28.679	1.79438	28.65	1.80413	28.547	1.85872
32	1.97086	30.795	1.8126	30.764	1.90165	30.733	1.92115	30.662	1.97727
34.098	2.08261	32.814	1.90954	32.781	1.99917	32.535	2.04257	32.586	2.07187
36.129	2.1842	34.769	2.00646	34.734	2.09669	34.767	2.1569	34.176	2.16647
38.095	2.28579	36.661	2.10339	36.624	2.19421	36.546	2.25968	36.545	2.26108
40	2.38738	38.494	2.20033	38.455	2.29173	38.342	2.35437	38.39	2.36252
41.846	2.47881	40.271	2.27787	40.23	2.3795	39.766	2.45022	40.071	2.45726
43.636	2.57024	41.993	2.35542	41.951	2.46727	41.464	2.53337	41.632	2.56512
45.216	2.66081	43.665	2.42327	43.621	2.53553	43.616	2.62922	43.376	2.64859
47.035	2.74385	45.287	2.49112	45.242	2.6038	44.958	2.71814	45.062	2.72264
48.281	2.79777	46.863	2.55897	46.673	2.67786	46.56	2.79552	46.63	2.80127
50.29	2.87541	48.393	2.62682	48.161	2.74724	48.295	2.85735	48.153	2.87991
52.108	2.92286	49.941	2.67922	49.472	2.81554	49.778	2.92562	49.692	2.94237
53.333	2.97661	51.325	2.74314	51.273	2.8671	51.221	2.99388	51.361	3.002
54.795	3.03756	52.732	2.8013	52.679	2.92562	52.625	3.06215	52.684	3.06812
56.216	3.09852	54.114	2.85351	54.045	2.98413	53.99	3.13041	54.008	3.12775
57.6	3.15947	55.431	2.90792	55.375	3.04264	55.319	3.18892	55.256	3.18195
58.947	3.22043	56.728	2.95638	56.67	3.0914	56.613	3.24743	56.661	3.25613
60.26	3.27122	57.991	3.00485	57.933	3.14016	57.874	3.29619	57.901	3.31312
61.538	3.32202	59.221	3.05332	59.161	3.18892	59.101	3.34495	59.126	3.37011
62.785	3.37281	60.421	3.10178	60.36	3.23768	60.299	3.39371	60.121	3.42051
64	3.42361	61.591	3.15025	61.528	3.28644	61.466	3.44248		
65.185	3.46424	62.731	3.18902	62.668	3.32545	62.604	3.48148		
				63.779	3.36446				

Table S13. Concentration-specific conductivity (κ) data of promethazine hydrochloride (PMH) in the presence of *p*-TDH (α_1)=1.08×10^{-4} in aqueous media at different temperatures

Temp=293.15 K		Temp=298.15 K		Temp=303.15 K		Temp=308.15 K		Temp=313.15 K	
Conc/ mmol·kg^{-1}	κ/ mS cm^{-1}	Conc/ mmol·kg^{-1}	κ/ mS cm^{-1}	Conc/ mmol·kg^{-1}	κ/ mS cm^{-1}	Conc/ mmol·kg^{-1}	κ/ mS cm^{-1}	Conc/ mmol·kg^{-1}	κ/ mS cm^{-1}
0	0	0	0	0	0	0	0	0	0
3.2	0.24528	3.6165	0.19055	3.5649	0.22559	3.2205	0.23453	3.2366	0.21904
6.5206	0.45278	6.427	0.37557	6.5462	0.43595	5.9929	0.42566	6.1526	0.4293
9.3376	0.65023	9.099	0.55265	8.9	0.6023	8.8827	0.60112	9.0542	0.61932
12.062	0.84826	12.173	0.7499	11.917	0.79651	11.525	0.80294	11.468	0.80927
14.792	1.02201	14.429	0.89581	14.076	0.9558	13.872	0.97805	14.064	0.97504
17.422	1.18552	16.918	1.03842	16.579	1.11993	16.368	1.13307	16.57	1.15411
19.757	1.36951	19.306	1.20476	18.99	1.26474	18.534	1.29568	19.055	1.3062
22.184	1.50186	21.557	1.33656	21.315	1.40956	21.248	1.45	21.126	1.44097
24.525	1.65157	23.826	1.46156	23.559	1.53507	23.346	1.55911	23.739	1.58587
27.034	1.74762	26.016	1.57694	25.725	1.66058	25.346	1.68486	25.81	1.6872
29.234	1.87026	28.134	1.69233	27.819	1.77644	27.677	1.8041	27.776	1.84385
31.36	1.98269	30.179	1.7981	29.841	1.88263	29.752	1.92444	29.882	1.93343
33.416	2.09511	32.158	1.89426	31.798	1.97918	31.662	2.03176	31.647	2.03375
35.406	2.19731	34.073	1.99041	33.692	2.07572	33.662	2.14558	33.565	2.14015
37.333	2.2995	35.928	2.08656	35.525	2.17227	35.406	2.24207	35.559	2.24299
39.2	2.4017	37.872	2.16649	37.302	2.26881	37.383	2.33554	37.707	2.3195
41.009	2.49368	39.692	2.24756	39.023	2.3557	38.771	2.43062	39.403	2.40361
42.763	2.58566	41.331	2.30025	40.692	2.4426	40.428	2.5131	41.168	2.49886
44.312	2.67677	42.88	2.37017	42.312	2.51017	42.525	2.60819	42.78	2.58296
46.094	2.76031	44.699	2.44008	43.884	2.57776	43.962	2.67894	44.628	2.67213
47.316	2.81456	46.263	2.50392	45.273	2.65108	45.541	2.75049	46.241	2.73901
49.284	2.89266	47.737	2.56269	46.716	2.71977	47.12	2.81662	47.769	2.8069
51.066	2.9404	49.03	2.62045	47.992	2.76637	48.534	2.88275	49.229	2.88492
52.266	2.99447	50.414	2.67314	49.735	2.83843	50.113	2.9543	50.382	2.93559
53.699	3.05579	51.977	2.74914	51.098	2.89636	51.692	3.02584	51.842	2.9974
55.092	3.11711	53.526	2.79575	52.424	2.95429	52.774	3.08655	53.079	3.0582
56.448	3.17843	54.564	2.85351	53.714	3.01221	53.932	3.13425	54.76	3.13116
57.768	3.23975	55.857	2.9062	54.97	3.06049	55.09	3.19387		
59.055	3.29085	57.165	2.9589	56.195	3.10876	56.594	3.24808		
60.307	3.34195	58.293	2.99943	57.387	3.15703	57.677	3.3077		
61.529	3.39305	59.586	3.05212	58.549	3.2053	58.791	3.36656		
62.72	3.44415					59.929	3.41494		
63.881	3.48503								

Table S14. Concentration-specific conductivity (κ) data of promethazine hydrochloride (PMH) in the presence of *p*-TDH (α_1)=1.44×10^{-4} in aqueous media at different temperatures

Temp=293.15 K		Temp=298.15 K		Temp=303.15 K		Temp=308.15 K		Temp=313.15 K	
Conc/ mmol·kg^{-1}	κ/ mS cm^{-1}	Conc/ mmol·kg^{-1}	κ/ mS cm^{-1}	Conc/ mmol·kg^{-1}	κ/ mS cm^{-1}	Conc/ mmol·kg^{-1}	κ/ mS cm^{-1}	Conc/ mmol·kg^{-1}	κ/ mS cm^{-1}
0	0	0	0	0	0	0	0	0	0
3.5486	0.24318	3.5514	0.18903	3.0166	0.20778	3.1593	0.23312	3.146	0.21543
6.8324	0.449124	6.3113	0.37257	6.3629	0.43159	5.879	0.42311	5.9803	0.42222
9.7841	0.644989	8.9352	0.54823	8.6508	0.59628	8.6872	0.60094	8.8007	0.6091
12.639	0.841416	11.954	0.7439	11.584	0.78854	11.306	0.79812	11.147	0.79592
15.383	1.013442	14.169	0.88864	13.682	0.94624	13.609	0.97218	13.67	0.95895
17.596	1.173599	16.414	1.0388	16.114	1.10873	16.057	1.12627	16.106	1.13507
19.481	1.264029	18.414	1.16321	18.138	1.26263	18.182	1.28791	18.522	1.28465
22.333	1.440517	20.759	1.29988	20.292	1.41969	20.845	1.4413	20.535	1.41719
25.578	1.617015	22.699	1.41864	22.447	1.53115	22.902	1.54976	23.074	1.5597
28.086	1.745574	24.564	1.51101	25.005	1.64397	24.864	1.67475	25.087	1.65936
30.632	1.85518	27.797	1.65993	27.04	1.75868	27.151	1.79328	27.351	1.79283
33.052	1.960202	29.797	1.74853	29.006	1.8638	29.187	1.91289	29.046	1.90153
35.036	2.049547	32.053	1.84844	30.907	1.95939	31.06	2.01957	31.089	1.99076
37.593	2.16285	33.782	1.9295	32.748	2.05496	33.26	2.11279	33.054	2.07371
39.478	2.245652	35.692	2.00679	34.53	2.15055	35.261	2.20196	34.892	2.17267
41.756	2.348062	37.857	2.09067	36.609	2.23033	37.095	2.28606	36.869	2.26693
43.346	2.428683	39.767	2.16513	38.527	2.3114	38.861	2.37017	38.413	2.33385
45.657	2.506038	41.541	2.2264	39.959	2.37625	40.556	2.45427	40.174	2.4281
47.591	2.595372	43	2.29049	41.724	2.47454	42.321	2.52723	41.73	2.50633
49.427	2.692335	44.91	2.35741	42.919	2.54446	44.003	2.60525	43.287	2.57891
50.886	2.765338	46.579	2.42716	44.517	2.59715	45.24	2.67213	45.252	2.6628
52.525	2.839416	48.399	2.4856	45.796	2.64984	46.546	2.73394	46.668	2.74574
53.672	2.887355	49.602	2.54121	47.241	2.71976	48.228	2.81805	47.931	2.8136
54.984	2.951635	51.15	2.60719	48.84	2.78967	49.618	2.88492	49.271	2.8711
56.77	3.009382	52.654	2.66845	50.118	2.84237	51.23	2.95788	50.687	2.92765
58.163	3.080194	54.068	2.71841	51.23	2.9062	52.759	3.01969		
		55.541	2.77402	52.509	2.96498	53.843	3.07543		
		56.729	2.81832	53.801	3.01159	55.302	3.13116		
				55.233	3.06935	56.678	3.19905		

Table S15. Concentration-specific conductivity (κ) data of promethazine hydrochloride (PMH) in the presence of *p*-TDH (α_1)=1.80×10^{-4} in aqueous media at different temperatures

Temp=293.15 K		Temp=298.15 K		Temp=303.15 K		Temp=308.15 K		Temp=313.15 K	
Conc/ mmol·kg^{-1}	κ/ mS cm^{-1}	Conc/ mmol·kg^{-1}	κ/ mS cm^{-1}	Conc/ mmol·kg^{-1}	κ/ mS cm^{-1}	Conc/ mmol·kg^{-1}	κ/ mS cm^{-1}	Conc/ mmol·kg^{-1}	κ/ mS cm^{-1}
0	0	0	0	0	0	0	0	0	0
3.2556	0.24197	3.5865	0.22251	2.6874	0.18768	3.0803	0.23102	3.0862	0.21349
6.2683	0.44689	5.977	0.39861	5.6986	0.3941	5.7321	0.4193	5.8667	0.41842
8.9762	0.64178	8.6939	0.5411	8.1994	0.55622	8.3814	0.61088	8.3142	0.58449
11.595	0.83723	11.631	0.73423	10.254	0.71362	11.023	0.79094	10.713	0.7353
14.113	1.0084	13.786	0.87709	12.818	0.87668	13.268	0.96343	12.818	0.89176
16.143	1.16776	15.97	1.0253	14.515	1.00675	15.656	1.11613	14.796	1.0322
17.872	1.25774	17.818	1.12567	16.199	1.13117	17.727	1.27632	16.557	1.14153
20.489	1.43335	19.486	1.24598	18.037	1.24993	20.323	1.42833	19.593	1.31402
23.466	1.60897	21.168	1.32618	19.721	1.34795	22.33	1.53581	22.196	1.45446
25.767	1.73689	24.212	1.47613	22.579	1.52138	24.243	1.65968	24.952	1.5949
28.103	1.84595	26.449	1.57638	24.71	1.63543	26.472	1.77714	27.07	1.70423
30.323	1.95045	29.563	1.67664	27.134	1.75419	28.645	1.86541	29.112	1.80791
32.143	2.03935	31.647	1.7673	29.265	1.86823	30.257	1.94929	31.089	1.90217
34.489	2.15209	33.718	1.84751	31.612	1.97663	32.565	2.069	33.195	1.99548
36.218	2.23448	36.206	1.94253	33.743	2.09633	34.483	2.16796	35.172	2.09444
38.308	2.33638	37.804	2.01314	35.797	2.18304	36.331	2.24619	36.729	2.15759
39.767	2.4166	39.166	2.06284	37.418	2.28012	38.013	2.34516	38.132	2.24054
41.887	2.49357	40.848	2.11776	39.026	2.35082	39.555	2.40737	40.314	2.33385
43.662	2.58246	42.599	2.17791	40.493	2.42151	41.263	2.50448	41.73	2.40171
45.346	2.67894	44.114	2.24329	41.743	2.48654	42.71	2.56854	43.427	2.49031
46.684	2.75158	46.116	2.31391	43.287	2.55629	44.17	2.64677	44.971	2.56854
48.188	2.82529	47.881	2.38365	44.468	2.61804	45.546	2.70898	46.451	2.63641
49.241	2.87299	49.312	2.43421	45.871	2.68712	47.241	2.77684	47.931	2.71935
50.444	2.93695	50.758	2.49437	47.423	2.75619	48.534	2.84942	49.207	2.77684
52.083	2.99441	52.509	2.56934	48.665	2.80826	49.949	2.93126		
53.361	3.06487	54.19	2.62426	49.744	2.87133				
		55.4	2.68006						